

UNIVERSIDAD DE CONCEPCIÓN



CENTRO DE INVESTIGACIÓN EN
INGENIERÍA MATEMÁTICA (CI²MA)



Mixed displacement-rotation-pressure formulations for elasticity

VERONICA ANAYA, ZOA DE WIJN,
DAVID MORA, RICARDO RUIZ-BAIER

PREPRINT 2017-12

SERIE DE PRE-PUBLICACIONES

Mixed displacement-rotation-pressure formulations for elasticity

VERÓNICA ANAYA,^{*} ZOA DE WIJN,[‡] DAVID MORA,^{*,†} RICARDO RUIZ-BAIER[‡]

Abstract

We propose a family of mixed finite element and finite volume element methods for the approximation of linear elastostatics, formulated in terms of displacement, rotation vector, and pressure. The unique solvability of the three-field continuous formulation, as well as the invertibility and stability of the proposed Galerkin and Petrov-Galerkin methods, is established thanks to the Babuška-Brezzi theory. Optimal a priori error estimates are derived using norms robust with respect to the Lamé constants, turning these numerical methods particularly appealing for nearly incompressible materials. We exemplify the accuracy and applicability of the new formulation and the mixed schemes by conducting a number of computational tests in 2D and 3D.

Key words: Elasticity equations; rotation vector; mixed finite elements; finite volume element formulation; error analysis

Mathematics subject classifications (2000): 65N30, 65N12, 76D07, 65N15

1 Introduction

The numerical solution of elasticity-based problems encompasses well-documented difficulties. For instance, for pure-displacement formulations, if one uses classical finite element discretisations based on piecewise linear and continuous elements, then accuracy is ensured only for moderate values of the Poisson ratio ν . As $\nu \rightarrow 0.5$ (that is, when the Lamé constant $\lambda \rightarrow \infty$ and the elastic material becomes nearly incompressible), the numerical scheme might generate spurious solutions (unphysically small deformations referred to as locking phenomenon, see for instance [9]). A number of alternative formulations and associated numerical methods are available to overcome this issue. Notably, choosing a mixed scheme would produce accurate solutions even for nearly incompressible materials, and at the same time, one accommodates the direct approximation of auxiliary variables of interest such as pressure, stress, or rotations.

One of the most commonly used mixed approaches for linear elasticity is the Hu-Washizu formulation [25, 45]. Some popular methods based on the Hu-Washizu formulation include the enhanced assumed strain method [42], the assumed stress method [38], the mixed-enhanced strain method [28], the strain gap method [40], and the so-called B-bar method [26]. Some of these methods actually coincide under certain conditions (see the discussions in e.g. [1, 10, 15]). The well-posedness for this class of formulations has been established in [33], where it is also shown that a modified version of the Hu-Washizu formulation is more amenable for obtaining uniform convergence with respect to the model parameters when approaching the incompressibility limit. Alternatively, other mixed formulations (such as the Hellinger-Reissner principle) can be employed to obtain robust methods with respect to the Lamé constants.

^{*}GIMNAP, Departamento de Matemática, Universidad del Bío-Bío, Casilla 5-C, Concepción, Chile. E-mail: {vanaya,dmora}@ubiobio.cl.

[†]Centro de Investigación en Ingeniería Matemática (CI²MA), Universidad de Concepción, Concepción, Chile.

[‡]Mathematical Institute, University of Oxford, A. Wiles Building, Woodstock Road, Oxford OX2 6GG, UK. E-mail: {dewijn,ruizbaier}@maths.ox.ac.uk.

Schemes more closely related to the present contribution deal with mixed formulations for elasticity involving pressure, stress, and rotation. We mention for instance mixed formulations based on stress [3, 4, 7, 8], the augmented scheme in [22], a family of pseudostress-based methods from [20, 21], the displacement-pressure mixed formulations [9, 11]; and the first-order least squares presented in [12]. We also mention locking-free methods for plate models [6], and the membrane elements introduced in [27], all including rotation tensors as an additional field.

In contrast to the brief literature survey given above, here we advocate to the formulation of the elasticity equations in terms of displacement, *rotation vector*, and pressure. It is worth noticing that the present three-field formulation has a resemblance with the displacement, pressure, and vorticity momentum formulations for acoustic fluid-structure interaction studied in [43, 44]. However in these two contributions the system is solved for the fluid displacement, and the vorticity momentum arises as the Lagrange multiplier imposing an irrotationality constraint.

In our case, after regarding the pressure together with the rotation vector as a single auxiliary unknown (defined in an appropriate product functional space), we are able to analyse the solvability of the resulting mixed variational formulation using the classical Babuška-Brezzi theory for saddle-point problems. Thanks to a rescaling of the rotation vector norm, the well-posedness result and the continuous dependence on the data turn out to be independent of the Lamé constants. Concerning numerical approximation, we first introduce a family of finite elements given by piecewise continuous polynomials of degree $k \geq 1$ for the displacement, and piecewise polynomials of degree $k - 1$ for the rotation and pressure. The unique solvability of the finite element scheme is then established using analogous techniques as in the continuous case. In addition, we prove optimal *a priori* error estimates with constants fully independent of the Lamé coefficient λ ; guaranteeing robustness of the method also in the nearly incompressible limit. We remark that in the two-dimensional case, the computational cost of the proposed finite element method in its lowest order configuration is $6|\mathcal{N}_h|$ (where \mathcal{N}_h denotes the set of vertices in the mesh and $|\mathcal{N}_h|$ its cardinality), which is lower than, for instance, the MINI element for displacement-pressure formulations (accounting for $7|\mathcal{N}_h|$ local degrees of freedom). These features turn the proposed discretisation into a very appealing method.

A further goal in this contribution is to employ the three-field formulation and the aforementioned finite element discretisation, to construct a finite volume element (FVE) method specifically tailored for elasticity equations. FVE schemes correspond to Petrov-Galerkin formulations where the trial space is constructed using a primal partition of the domain, whereas the test space is associated with either a dual mesh or a dual basis. Depending on the particular kind of dual grid, the transfer operator between trial and test spaces possesses different interpolation properties which are used in recasting a preliminary pure finite volume formulation into a Petrov-Galerkin one. In general, these methods enjoy some features shared by finite element and finite volume schemes, including local flux conservation properties, liberty to choose different numerical fluxes and dual partitions associated to unstructured primal meshes; and several others (see for example [13]). Discretisation schemes following this principle have been systematically employed in numerous fluid flow problems, including Stokes, Navier-Stokes (see e.g. [24, 34, 36, 39, 46]) and also in coupled flow-transport systems arising from diverse applications (see [16, 17, 41]). However, up to our knowledge, the only contributions addressing FVE-like discretisations for solid mechanics are the hybrid-stress finite volume method for linear elasticity on quads studied in [47]; and [31], where two alternative stabilisation approaches based on nodal pressure and dual bases and meshes are applied to construct inf-sup stable approximations for nearly incompressible linear elasticity. The class of finite volume element methods we introduce here is based on the lowest-order mixed finite element method discussed above. As in well-established FVE schemes for Stokes equations (*cf.* [34, 39]), it turns out that the two schemes differ only by the assembly of the forcing term, and therefore straightforward derivation of stability properties and energy estimates in natural norms can be done exploiting the results obtained for the family of mixed finite elements. In addition, the FVE scheme features mass conservativity on the dual control volumes, suitability for irregular domains and unstructured partitions, and robust approximations of displacements.

Outline. We have structured the contents of the manuscript in the following manner. A few recurrent notations and useful identities are recalled in the remainder of this section. In Section 2 we state the precise form of the linear elasticity equations that we will focus on, and we derive a suitable mixed weak formulation, and provide its solvability analysis. A Galerkin method is introduced in Section 3, where we also obtain stability properties and *a priori* error estimates. Section 4 concentrates on the development of a low-order finite volume element scheme, and its accuracy is studied in connection with the properties of the finite element method. The convergence and robustness of the proposed methods is illustrated via a set of insightful computational tests collected in Section 5. Finally, we present a variational formulation considering mixed boundary conditions in the Appendix.

Preliminaries. Let $d = 2, 3$ denote spatial dimension. For given vector fields $\boldsymbol{\theta} = (\theta_i)_{i=1}^d$, $\mathbf{v} = (v_i)_{i=1}^d$ we recall the following notation for differential operators:

$$\operatorname{div} \mathbf{v} := \partial_1 v_1 + \partial_2 v_2 + \partial_3 v_3, \quad \boldsymbol{\theta} \times \mathbf{v} := \begin{pmatrix} \theta_2 v_3 - \theta_3 v_2 \\ \theta_3 v_1 - \theta_1 v_3 \\ \theta_1 v_2 - \theta_2 v_1 \end{pmatrix}, \quad \operatorname{curl} \mathbf{v} := \nabla \times \mathbf{v} = \begin{pmatrix} \partial_2 v_3 - \partial_3 v_2 \\ \partial_3 v_1 - \partial_1 v_3 \\ \partial_1 v_2 - \partial_2 v_1 \end{pmatrix}.$$

We also recall a version of Green's formula given in e.g. [23, Theorem 2.11]:

$$\int_{\Omega} \operatorname{curl} \boldsymbol{\omega} \cdot \mathbf{v} = \int_{\Omega} \boldsymbol{\omega} \cdot \operatorname{curl} \mathbf{v} + \langle \boldsymbol{\omega} \times \mathbf{n}, \mathbf{v} \rangle_{\partial\Omega}, \quad (1.1)$$

and the following useful identity

$$\operatorname{curl}(\operatorname{curl} \mathbf{v}) = -\Delta \mathbf{v} + \nabla(\operatorname{div} \mathbf{v}). \quad (1.2)$$

2 The model problem

2.1 Derivation of a displacement-rotation-pressure formulation

We assume that an isotropic and linearly elastic solid occupies a bounded and connected Lipschitz domain Ω of \mathbb{R}^d , with boundary $\partial\Omega$. Determining the deformation of a linearly elastic body subject to a volume load and with given boundary conditions, and adopting the hypothesis of small strains, results in the classical linear elasticity problem, formulated as follows. Given an external force $\tilde{\mathbf{f}}$ and a prescribed boundary motion \mathbf{g} , we seek the displacements \mathbf{u} such that

$$\operatorname{div}(2\mu\boldsymbol{\varepsilon}(\mathbf{u}) + \lambda \operatorname{div} \mathbf{u} \mathbf{I}) = -\tilde{\mathbf{f}} \text{ in } \Omega, \quad \mathbf{u} = \mathbf{g} \text{ on } \partial\Omega, \quad (2.1)$$

where $\boldsymbol{\varepsilon}(\mathbf{u}) = \frac{1}{2}(\nabla \mathbf{u} + \nabla \mathbf{u}^\top)$ is the infinitesimal strain tensor, \mathbf{I} denotes the $d \times d$ -identity matrix, and μ, λ are the Lamé coefficients (intrinsic to the material properties of the solid, and here assumed constant).

Next, and following the pseudostress-based formulation recently introduced in [21] (and motivated by the seminal work [3]), one notices that using the identity

$$\operatorname{div}(\boldsymbol{\varepsilon}(\mathbf{u})) = \frac{1}{2}\Delta \mathbf{u} + \frac{1}{2}\nabla(\operatorname{div} \mathbf{u}),$$

and dividing the momentum equation by $\lambda + \mu$, we can rewrite (2.1) in the form of the well-known Cauchy-Navier (or Navier-Lamé) equations

$$\frac{\mu}{\lambda + \mu}\Delta \mathbf{u} + \nabla(\operatorname{div} \mathbf{u}) = -\mathbf{f} \text{ in } \Omega, \quad \mathbf{u} = \mathbf{g} \text{ on } \partial\Omega, \quad (2.2)$$

where the right hand side has been rescaled as $\mathbf{f} = \frac{1}{\lambda+\mu}\tilde{\mathbf{f}}$. We then proceed to define the auxiliary scaling parameter $\eta := \frac{\mu}{\lambda+\mu} > 0$, and recast (2.2) in a displacement-pressure formulation (considering $p = -\operatorname{div} \mathbf{u}$ as the solid pressure) as follows

$$\begin{aligned} \eta \Delta \mathbf{u} - \nabla p &= -\mathbf{f} && \text{in } \Omega, \\ \operatorname{div} \mathbf{u} + p &= 0 && \text{in } \Omega, \\ \mathbf{u} &= \mathbf{g} && \text{on } \partial\Omega. \end{aligned} \tag{2.3}$$

At this point, and with the aim of deriving formulations whose stability holds independently of the Lamé coefficient λ , we introduce the field of rescaled rotations $\boldsymbol{\omega} := \sqrt{\eta} \operatorname{curl} \mathbf{u}$, as an additional unknown in the problem. Exploiting (1.2) and the definition of pressure in terms of displacements, we observe that (2.3) is fully equivalent to the following set of governing equations, in their pure-Dirichlet case. Find the displacement \mathbf{u} , the rotation $\boldsymbol{\omega}$ and the pressure p such that (see [12]):

$$\sqrt{\eta} \operatorname{curl} \boldsymbol{\omega} + (1 + \eta) \nabla p = \mathbf{f} \quad \text{in } \Omega, \tag{2.4}$$

$$\boldsymbol{\omega} - \sqrt{\eta} \operatorname{curl} \mathbf{u} = 0 \quad \text{in } \Omega, \tag{2.5}$$

$$\operatorname{div} \mathbf{u} + p = 0 \quad \text{in } \Omega, \tag{2.6}$$

$$\mathbf{u} = \mathbf{g} \quad \text{on } \partial\Omega. \tag{2.7}$$

On the other hand, should one necessitate to incorporate mixed boundary conditions, to e.g. impose a displacement \mathbf{g} only on a part of the boundary Γ_D , and set a given traction $\tilde{\mathbf{t}}$ on the remainder of the boundary, say $\Gamma_N = \partial\Omega \setminus \Gamma_D$, we can proceed as follows. First we realise that $\boldsymbol{\varepsilon}(\mathbf{u})\mathbf{n} = (\nabla \mathbf{u})\mathbf{n} - \frac{1}{2} \operatorname{curl} \mathbf{u} \times \mathbf{n}$ (where \mathbf{n} denotes the outward unit normal on the boundary). Then, thanks to (2.1) and (2.4), the normal Cauchy stress can be recast in terms of the strain, rotations and pressure, and so the following set of mixed boundary conditions can be used instead of (2.7):

$$\mathbf{u} = \mathbf{g} \text{ on } \Gamma_D, \quad \text{and} \quad 2\eta(\nabla \mathbf{u})\mathbf{n} - \sqrt{\eta} \boldsymbol{\omega} \times \mathbf{n} - (1 - \eta)p\mathbf{n} = \mathbf{t} \text{ on } \Gamma_N, \tag{2.8}$$

where the rescaled traction is $\mathbf{t} = \frac{1}{\lambda+\mu}\tilde{\mathbf{t}}$. However, and for sake of clarity, we will restrict the presentation and analysis to the pure Dirichlet case $\Gamma_D \equiv \partial\Omega$, considering only clamped boundaries $\mathbf{g} = \mathbf{0}$. A brief comment on how (2.8) is set up in a mixed variational formulation is postponed to the Appendix.

2.2 Weak form of the governing equations

Let us introduce the functional spaces

$$\mathbf{H} := \mathbf{H}_0^1(\Omega)^d, \quad \mathbf{Z} := \mathbf{L}^2(\Omega)^d, \quad \text{and} \quad \mathbf{Q} := \mathbf{L}^2(\Omega),$$

where \mathbf{Z} and \mathbf{Q} are endowed with their natural norms, and we recall the definition of the norm in the product space $\mathbf{Z} \times \mathbf{Q}$ as

$$\|(\boldsymbol{\theta}, q)\|_{\mathbf{Z} \times \mathbf{Q}}^2 := \|\boldsymbol{\theta}\|_{0,\Omega}^2 + \|q\|_{0,\Omega}^2.$$

On the other hand, for \mathbf{H} we consider the following η -dependent scaled norm (see for instance, [23, Remark 2.7]):

$$\|\mathbf{v}\|_{\mathbf{H}}^2 := \eta \|\operatorname{curl} \mathbf{v}\|_{0,\Omega}^2 + \|\operatorname{div} \mathbf{v}\|_{0,\Omega}^2,$$

We proceed to test (2.6) against adequate functions, to integrate by parts in two terms, and to take into account the boundary conditions (2.7) in such a way that the resulting mixed variational formulation reads as follows. Find $((\boldsymbol{\omega}, p), \mathbf{u}) \in (\mathbf{Z} \times \mathbf{Q}) \times \mathbf{H}$ such that

$$\int_{\Omega} \boldsymbol{\omega} \cdot \boldsymbol{\theta} + (1 + \eta) \int_{\Omega} pq + (1 + \eta) \int_{\Omega} q \operatorname{div} \mathbf{u} - \sqrt{\eta} \int_{\Omega} \boldsymbol{\theta} \cdot \operatorname{curl} \mathbf{u} = 0 \quad \forall (\boldsymbol{\theta}, q) \in \mathbf{Z} \times \mathbf{Q},$$

$$(1 + \eta) \int_{\Omega} p \operatorname{div} \mathbf{v} - \sqrt{\eta} \int_{\Omega} \boldsymbol{\omega} \cdot \operatorname{curl} \mathbf{v} = - \int_{\Omega} \mathbf{f} \cdot \mathbf{v} \quad \forall \mathbf{v} \in \mathbf{H}.$$

Introducing the bilinear forms $a : (\mathbf{Z} \times \mathbf{Q}) \times (\mathbf{Z} \times \mathbf{Q}) \rightarrow \mathbb{R}$, $b : (\mathbf{Z} \times \mathbf{Q}) \times \mathbf{H} \rightarrow \mathbb{R}$, together with the linear functional $F : \mathbf{H} \rightarrow \mathbb{R}$, all defined as

$$\begin{aligned} a((\boldsymbol{\omega}, p), (\boldsymbol{\theta}, q)) &:= \int_{\Omega} \boldsymbol{\omega} \cdot \boldsymbol{\theta} + (1 + \eta) \int_{\Omega} pq, \\ b((\boldsymbol{\theta}, q), \mathbf{v}) &:= (1 + \eta) \int_{\Omega} q \operatorname{div} \mathbf{v} - \sqrt{\eta} \int_{\Omega} \boldsymbol{\theta} \cdot \operatorname{curl} \mathbf{v}, \\ F(\mathbf{v}) &:= - \int_{\Omega} \mathbf{f} \cdot \mathbf{v}, \end{aligned}$$

for all $\mathbf{v} \in \mathbf{H}$, $\boldsymbol{\omega}, \boldsymbol{\theta} \in \mathbf{Z}$, and $p, q \in \mathbf{Q}$; we realise that the variational problem above can be recast as: Find $((\boldsymbol{\omega}, p), \mathbf{u}) \in (\mathbf{Z} \times \mathbf{Q}) \times \mathbf{H}$ such that

$$a((\boldsymbol{\omega}, p), (\boldsymbol{\theta}, q)) + b((\boldsymbol{\theta}, q), \mathbf{u}) = 0 \quad \forall (\boldsymbol{\theta}, q) \in \mathbf{Z} \times \mathbf{Q}, \quad (2.9)$$

$$b((\boldsymbol{\omega}, p), \mathbf{v}) = F(\mathbf{v}) \quad \forall \mathbf{v} \in \mathbf{H}. \quad (2.10)$$

2.3 Well-posedness

The unique solvability of problem (2.9)-(2.10), together with the continuous dependence on the data will be established using the well-known Babuška-Brezzi theory.

We first observe that the bilinear forms $a(\cdot, \cdot)$, $b(\cdot, \cdot)$ and the linear functional $F(\cdot)$ are all bounded by positive constants independent of η (and therefore independent of the Lamé coefficient λ). In addition, the bilinear form $a(\cdot, \cdot)$ is $(\mathbf{Z} \times \mathbf{Q})$ -elliptic, uniformly with respect to the scaling parameter η , as stated in the following result.

Lemma 2.1 *There exists $\alpha > 0$, independent of η , such that*

$$a((\boldsymbol{\theta}, q), (\boldsymbol{\theta}, q)) \geq \alpha \|(\boldsymbol{\theta}, q)\|_{\mathbf{Z} \times \mathbf{Q}}^2 \quad \forall (\boldsymbol{\theta}, q) \in \mathbf{Z} \times \mathbf{Q}.$$

Moreover, an inf-sup condition holds for the bilinear form $b(\cdot, \cdot)$.

Lemma 2.2 *There exists $C > 0$, independent of η , such that*

$$\sup_{(\boldsymbol{\theta}, q) \in \mathbf{Z} \times \mathbf{Q}} \frac{b((\boldsymbol{\theta}, q), \mathbf{v})}{\|(\boldsymbol{\theta}, q)\|_{\mathbf{Z} \times \mathbf{Q}}} \geq C \|\mathbf{v}\|_{\mathbf{H}} \quad \forall \mathbf{v} \in \mathbf{H}.$$

Proof. Let us consider a generic $\mathbf{v} \in \mathbf{H}$ and define

$$\tilde{\boldsymbol{\theta}} := -\sqrt{\eta} \operatorname{curl} \mathbf{v} \in \mathbf{Z}, \quad \text{and} \quad \tilde{q} := \operatorname{div} \mathbf{v} \in \mathbf{Q}.$$

We immediately notice that

$$\|(\tilde{\boldsymbol{\theta}}, \tilde{q})\|_{\mathbf{Z} \times \mathbf{Q}} \leq \|\mathbf{v}\|_{\mathbf{H}},$$

and from the definition of $b(\cdot, \cdot)$, we readily obtain

$$\sup_{(\boldsymbol{\theta}, q) \in \mathbf{Z} \times \mathbf{Q}} \frac{b((\boldsymbol{\theta}, q), \mathbf{v})}{\|(\boldsymbol{\theta}, q)\|_{\mathbf{Z} \times \mathbf{Q}}} \geq \frac{b((\tilde{\boldsymbol{\theta}}, \tilde{q}), \mathbf{v})}{\|(\tilde{\boldsymbol{\theta}}, \tilde{q})\|_{\mathbf{Z} \times \mathbf{Q}}} \geq C \|\mathbf{v}\|_{\mathbf{H}} \quad \forall \mathbf{v} \in \mathbf{H},$$

which finishes the proof. \square

We are now in a position to state the solvability of the continuous problem (2.9)-(2.10).

Theorem 2.1 *There exists a unique solution $((\boldsymbol{\omega}, p), \mathbf{u}) \in (\mathbf{Z} \times \mathbf{Q}) \times \mathbf{H}$ to problem (2.9)-(2.10), which satisfies the following continuous dependence on the data*

$$\|(\boldsymbol{\omega}, p)\|_{\mathbf{Z} \times \mathbf{Q}} + \|\mathbf{u}\|_{\mathbf{H}} \leq C \|\mathbf{f}\|_{0, \Omega}.$$

Proof. By virtue of the general theory for saddle-point problems (see e.g. [19]), the desired result follows from a direct application of Lemmas 2.1 and 2.2. \square

3 Finite element discretisation

In this section, we introduce a Galerkin scheme associated to problem (2.9)-(2.10), we specify the finite dimensional subspaces to employ, and analyse the well-posedness of the resulting methods using suitable assumptions on the discrete spaces. The section also contains a derivation of error estimates.

3.1 Formulation and solvability

Let $\{\mathcal{T}_h(\Omega)\}_{h>0}$ be a shape-regular family of partitions of the domain Ω , by tetrahedrons (if $d = 3$, or triangles if $d = 2$) T of diameter h_T , having meshsize $h := \max\{h_T : T \in \mathcal{T}_h(\Omega)\}$. Given an integer $k \geq 1$ and a set $S \subset \mathbb{R}^d$, the space of polynomial functions defined in S and having total degree $\leq k$ will be denoted by $\mathcal{P}_k(S)$.

Next, we define the following discrete spaces:

$$\begin{aligned} \mathbf{H}_h &:= \{\mathbf{v}_h \in \mathbf{H} : \mathbf{v}_h|_T \in \mathcal{P}_k(T)^d \quad \forall T \in \mathcal{T}_h(\Omega)\}, \\ \mathbf{Z}_h &:= \{\boldsymbol{\theta}_h \in \mathbf{Z} : \boldsymbol{\theta}_h|_T \in \mathcal{P}_{k-1}(T)^d \quad \forall T \in \mathcal{T}_h(\Omega)\}, \\ \mathbf{Q}_h &:= \{q_h \in \mathbf{Q} : q_h|_T \in \mathcal{P}_{k-1}(T) \quad \forall T \in \mathcal{T}_h(\Omega)\}, \end{aligned}$$

which are subspaces of \mathbf{H} , \mathbf{Z} and \mathbf{Q} , respectively; and proceed to state a Galerkin scheme associated to the continuous variational formulation (2.9)-(2.10). Find $((\boldsymbol{\omega}_h, p_h), \mathbf{u}_h) \in (\mathbf{Z}_h \times \mathbf{Q}_h) \times \mathbf{H}_h$ such that

$$a((\boldsymbol{\omega}_h, p_h), (\boldsymbol{\theta}_h, q_h)) + b((\boldsymbol{\theta}_h, q_h), \mathbf{u}_h) = 0 \quad \forall (\boldsymbol{\theta}_h, q_h) \in \mathbf{Z}_h \times \mathbf{Q}_h, \quad (3.1)$$

$$b((\boldsymbol{\omega}_h, p_h), \mathbf{v}_h) = F(\mathbf{v}_h) \quad \forall \mathbf{v}_h \in \mathbf{H}_h. \quad (3.2)$$

Our next goal is to establish discrete counterparts of Lemmas 2.1 and 2.2, leading to the solvability and stability of the Galerkin method (3.1)-(3.2). Their proofs are obtained using the same arguments exploited in the continuous case. For completeness we provide the essential steps of the latter result.

Lemma 3.1 *There exists $\alpha > 0$, independent of η , such that*

$$a((\boldsymbol{\theta}_h, q_h), (\boldsymbol{\theta}_h, q_h)) \geq \alpha \|(\boldsymbol{\theta}_h, q_h)\|_{\mathbf{Z} \times \mathbf{Q}}^2.$$

Lemma 3.2 *There exists $C > 0$, independent of η , such that*

$$\sup_{(\boldsymbol{\theta}_h, q_h) \in \mathbf{Z}_h \times \mathbf{Q}_h} \frac{b((\boldsymbol{\theta}_h, q_h), \mathbf{v}_h)}{\|(\boldsymbol{\theta}_h, q_h)\|_{\mathbf{Z} \times \mathbf{Q}}} \geq C \|\mathbf{v}_h\|_{\mathbf{H}} \quad \forall \mathbf{v}_h \in \mathbf{H}_h.$$

Proof. For a generic $\mathbf{v} \in \mathbf{H}_h$, let us define

$$\tilde{\boldsymbol{\theta}}_h := -\sqrt{\eta} \mathbf{curl} \mathbf{v}_h \in \mathbf{Z}_h, \quad \text{and} \quad \tilde{q}_h := \text{div} \mathbf{v}_h \in \mathbf{Q}_h.$$

Then we readily notice that

$$\|(\tilde{\boldsymbol{\theta}}_h, \tilde{q}_h)\|_{\mathbf{Z} \times \mathbf{Q}} \leq \|\mathbf{v}_h\|_{\mathbf{H}},$$

and so, from the definition of the bilinear form $b(\cdot, \cdot)$, we arrive at

$$\sup_{(\boldsymbol{\theta}_h, q_h) \in Z_h \times Q_h} \frac{b((\boldsymbol{\theta}_h, q_h), \mathbf{v}_h)}{\|(\boldsymbol{\theta}_h, q_h)\|_{Z \times Q}} \geq \frac{b((\tilde{\boldsymbol{\theta}}_h, \tilde{q}_h), \mathbf{v}_h)}{\|(\tilde{\boldsymbol{\theta}}_h, \tilde{q}_h)\|_{Z \times Q}} \geq C \|\mathbf{v}_h\|_{\mathbf{H}} \quad \forall \mathbf{v}_h \in \mathbf{H}_h,$$

which finishes the proof. \square

We can now state the unique solvability, stability, and convergence properties of the discrete problem (3.1)-(3.2), formulated in form of the three following theorems.

Theorem 3.1 *There exists a unique $((\boldsymbol{\omega}_h, p_h), \mathbf{u}_h) \in (Z_h \times Q_h) \times \mathbf{H}_h$ solution of the discrete problem (3.1)-(3.2). Moreover, there exists a constant $C > 0$, independent of h and η , such that*

$$\|(\boldsymbol{\omega}_h, p_h)\|_{Z \times Q} + \|\mathbf{u}_h\|_{\mathbf{H}} \leq C \|\mathbf{f}\|_{0, \Omega}.$$

In addition, the following approximation property is satisfied

$$\|(\boldsymbol{\omega} - \boldsymbol{\omega}_h, p - p_h)\|_{Z \times Q} + \|\mathbf{u} - \mathbf{u}_h\|_{\mathbf{H}} \leq C \inf_{((\boldsymbol{\theta}_h, q_h), \mathbf{v}_h) \in (Z_h \times Q_h) \times \mathbf{H}_h} \|(\boldsymbol{\omega} - \boldsymbol{\theta}_h, p - q_h)\|_{Z \times Q} + \|\mathbf{u} - \mathbf{v}_h\|_{\mathbf{H}},$$

where $((\boldsymbol{\omega}, p), \mathbf{u}) \in (Z \times Q) \times \mathbf{H}$ is the unique solution of the mixed variational formulation (2.9)-(2.10).

Theorem 3.2 *Let $((\boldsymbol{\omega}, p), \mathbf{u}) \in (Z \times Q) \times \mathbf{H}$ and $((\boldsymbol{\omega}_h, p_h), \mathbf{u}_h) \in (Z_h \times Q_h) \times \mathbf{H}_h$ be the solutions of the continuous and discrete problems (2.9)-(2.10) and (3.1)-(3.2), respectively. Then*

$$\|(\boldsymbol{\omega} - \boldsymbol{\omega}_h, p - p_h)\|_{Z \times Q} + \|\mathbf{u} - \mathbf{u}_h\|_{\mathbf{H}} \leq Ch^k (\|\boldsymbol{\omega}\|_{k, \Omega} + \|p\|_{k, \Omega} + \|\mathbf{u}\|_{k+1, \Omega}).$$

Proof. The result follows from Theorem 3.1 and the standard error estimates for the Lagrange interpolant of \mathbf{u} and the vectorial and scalar L^2 -orthogonal projections for $\boldsymbol{\omega}$ and p , respectively. \square

To close this section, we observe that the convergence of the displacement approximation can be also measured in the $L^2(\Omega)^d$ -norm, thanks to a classical duality strategy.

Theorem 3.3 *Let $((\boldsymbol{\omega}, p), \mathbf{u}) \in (Z \times Q) \times \mathbf{H}$ and $((\boldsymbol{\omega}_h, p_h), \mathbf{u}_h) \in (Z_h \times Q_h) \times \mathbf{H}_h$ be the solutions of the continuous and discrete problems (2.9)-(2.10) and (3.1)-(3.2), respectively. Then, there exists a constant $C > 0$, independent of h and η , such that*

$$\|\mathbf{u} - \mathbf{u}_h\|_{0, \Omega} \leq Ch^{k+1} (\|\boldsymbol{\omega}\|_{k, \Omega} + \|p\|_{k, \Omega} + \|\mathbf{u}\|_{k+1, \Omega}).$$

Proof. Resorting to a duality argument, we first consider the following well posed problem: Find $((\boldsymbol{\xi}, \phi), \mathbf{z}) \in (Z \times Q) \times \mathbf{H}$ such that

$$a((\boldsymbol{\theta}, q), (\boldsymbol{\xi}, \phi)) + b((\boldsymbol{\theta}, q), \mathbf{z}) = 0 \quad \forall (\boldsymbol{\theta}, q) \in Z \times Q, \quad (3.3)$$

$$b((\boldsymbol{\xi}, \phi), \mathbf{v}) = \int_{\Omega} (\mathbf{u} - \mathbf{u}_h) \cdot \mathbf{v} \quad \forall \mathbf{v} \in \mathbf{H}. \quad (3.4)$$

We assume that the unique solution to (3.3)-(3.4) satisfies an additional regularity. More precisely, there exists a constant $\tilde{C} > 0$, independent of η such that

$$\|(\boldsymbol{\xi}, \phi)\|_{1, \Omega} + \|\mathbf{z}\|_{2, \Omega} \leq C \|\mathbf{u} - \mathbf{u}_h\|_{0, \Omega}. \quad (3.5)$$

Next, and thanks to (3.4), we observe that for all $(\boldsymbol{\xi}_h, \phi_h) \in Z_h \times Q_h$ we can write

$$\begin{aligned} \|\mathbf{u} - \mathbf{u}_h\|_{0, \Omega}^2 &= b((\boldsymbol{\xi}, \phi), \mathbf{u} - \mathbf{u}_h) \\ &= b((\boldsymbol{\xi} - \boldsymbol{\xi}_h, \phi - \phi_h), \mathbf{u} - \mathbf{u}_h) + b((\boldsymbol{\xi}_h, \phi_h), \mathbf{u} - \mathbf{u}_h) \\ &= b((\boldsymbol{\xi} - \boldsymbol{\xi}_h, \phi - \phi_h), \mathbf{u} - \mathbf{u}_h) - a((\boldsymbol{\omega} - \boldsymbol{\omega}_h, p - p_h), (\boldsymbol{\xi}_h, \phi_h)), \end{aligned} \quad (3.6)$$

where we have also employed (2.9) and (3.1). We then proceed to bound the second term in the right hand side of (3.6). This is carried out by adding and subtracting $(\boldsymbol{\xi}, \phi)$, and applying (3.3)

$$\begin{aligned} a((\boldsymbol{\omega} - \boldsymbol{\omega}_h, p - p_h), (\boldsymbol{\xi}_h, \phi_h)) &= a((\boldsymbol{\omega} - \boldsymbol{\omega}_h, p - p_h), (\boldsymbol{\xi}, \phi)) - a((\boldsymbol{\omega} - \boldsymbol{\omega}_h, p - p_h), (\boldsymbol{\xi} - \boldsymbol{\xi}_h, \phi - \phi_h)) \\ &= -b((\boldsymbol{\omega} - \boldsymbol{\omega}_h, p - p_h), \mathbf{z}) - a((\boldsymbol{\omega} - \boldsymbol{\omega}_h, p - p_h), (\boldsymbol{\xi} - \boldsymbol{\xi}_h, \phi - \phi_h)) \\ &= -b((\boldsymbol{\omega} - \boldsymbol{\omega}_h, p - p_h), \mathbf{z} - \mathbf{z}_h) - a((\boldsymbol{\omega} - \boldsymbol{\omega}_h, p - p_h), (\boldsymbol{\xi} - \boldsymbol{\xi}_h, \phi - \phi_h)), \end{aligned} \quad (3.7)$$

where in the last step we have also used (2.10) and (3.2), valid for all $\mathbf{z}_h \in \mathbf{H}_h$. Hence, from (3.6)-(3.7), we can deduce that

$$\begin{aligned} \|\mathbf{u} - \mathbf{u}_h\|_{0,\Omega}^2 &= \|(\boldsymbol{\xi} - \boldsymbol{\xi}_h, \phi - \phi_h)\|_{\mathbf{Z} \times \mathbf{Q}} \|\mathbf{u} - \mathbf{u}_h\|_{\mathbf{H}} + \|(\boldsymbol{\omega} - \boldsymbol{\omega}_h, p - p_h)\|_{\mathbf{Z} \times \mathbf{Q}} \|\mathbf{z} - \mathbf{z}_h\|_{\mathbf{H}} \\ &\quad + \|(\boldsymbol{\omega} - \boldsymbol{\omega}_h, p - p_h)\|_{\mathbf{Z} \times \mathbf{Q}} \|(\boldsymbol{\xi} - \boldsymbol{\xi}_h, \phi - \phi_h)\|_{\mathbf{Z} \times \mathbf{Q}}, \end{aligned}$$

which holds for all $(\boldsymbol{\xi}_h, \phi_h) \in \mathbf{Z}_h \times \mathbf{Q}_h$ and $\mathbf{z}_h \in \mathbf{H}_h$. Taking in particular the L^2 -orthogonal projections for $\boldsymbol{\xi}$ and ϕ and the Lagrange interpolant of \mathbf{z} in this last estimate, and using classical error estimates for the involved spaces together with the additional regularity (3.5), we finally obtain

$$\|\mathbf{u} - \mathbf{u}_h\|_{0,\Omega} \leq Ch^{k+1} (\|\boldsymbol{\omega}\|_{k,\Omega} + \|p\|_{k,\Omega} + \|\mathbf{u}\|_{k+1,\Omega}),$$

thus completing the proof. \square

4 A finite volume element scheme

In addition to the mesh \mathcal{T}_h (from now on, the primal mesh), we introduce another tessellation of Ω , denoted by \mathcal{T}_h^* and referred to as the *dual mesh*, where for each element $K \in \mathcal{T}_h$ we create segments joining its barycentre b_K with the midpoints (2D barycentres) m_F of each face $F \subset \partial K$ (or the midpoints of each edge, in 2D), forming four polyhedra (or three quadrilaterals, in the 2D case) Q_z for z in the set of vertices of K , that is, $z \in \mathcal{N}_h \cap K$. Then to each vertex $s_j \in \mathcal{N}_h$, we associate a so-called control volume K_j^* consisting of the union of the polyhedra (quadrilaterals in 2D) Q_{s_j} sharing the vertex s_j . A sketch of the resulting control volume associated to s_j is depicted in Figure 1(a).

In its lowest-order version, a FVE method for the approximation of (2.9)-(2.10) can be constructed by associating discrete spaces to a dual partition of the domain

$$\mathbf{H}_h^* := \{\mathbf{v} \in L^2(\Omega)^d : \mathbf{v}|_{K_j^*} \in \mathcal{P}_0(K_j^*)^d \text{ for all } K_j^* \in \mathcal{T}_h^*, \mathbf{v}|_{K_j^*} = \mathbf{0} \text{ if } K_j^* \text{ is a control volume on } \partial\Omega\},$$

and notice that no additional space is introduced for the finite volume approximation of $\boldsymbol{\omega}$ or p . Furthermore, we define the \mathcal{T}_h^* -piecewise lumping map $\mathcal{H}_h : \mathbf{H}_h \rightarrow \mathbf{H}_h^*$ which relates the primal and conforming dual meshes by

$$\mathbf{v}_h(\mathbf{x}) = \sum_j \mathbf{v}_h(s_j) \boldsymbol{\varphi}_j(\mathbf{x}) \mapsto \mathcal{H}_h \mathbf{v}_h(\mathbf{x}) = \sum_j \mathbf{v}_h(s_j) \boldsymbol{\chi}_j(\mathbf{x}),$$

for all $\mathbf{v}_h \in \mathbf{H}_h$, where $\boldsymbol{\chi}_j$ is the vectorial characteristic function of the control volume K_j^* and $\{\boldsymbol{\varphi}_j\}_j$ is the canonical FE basis of \mathbf{H}_h (cf. [39]). For any $\mathbf{v} \in \mathbf{H}$, this operator satisfies the interpolation bound (see e.g. [13])

$$\|\mathbf{v} - \mathcal{H}_h \mathbf{v}\|_{0,\Omega} \leq Ch \|\mathbf{v}\|_{1,\Omega}.$$

In addition, since $\mathbf{H} := \mathbf{H}_0^1(\Omega)^d = \mathbf{H}_0(\mathbf{curl}; \Omega) \cap \mathbf{H}_0(\text{div}; \Omega)$, remark [23, Remark 2.7] implies that the operator $\mathcal{H}_h(\cdot)$ also satisfies

$$\|\mathbf{v} - \mathcal{H}_h \mathbf{v}\|_{0,\Omega} \leq Ch \|\mathbf{v}\|_{\mathbf{H}}, \quad (4.1)$$

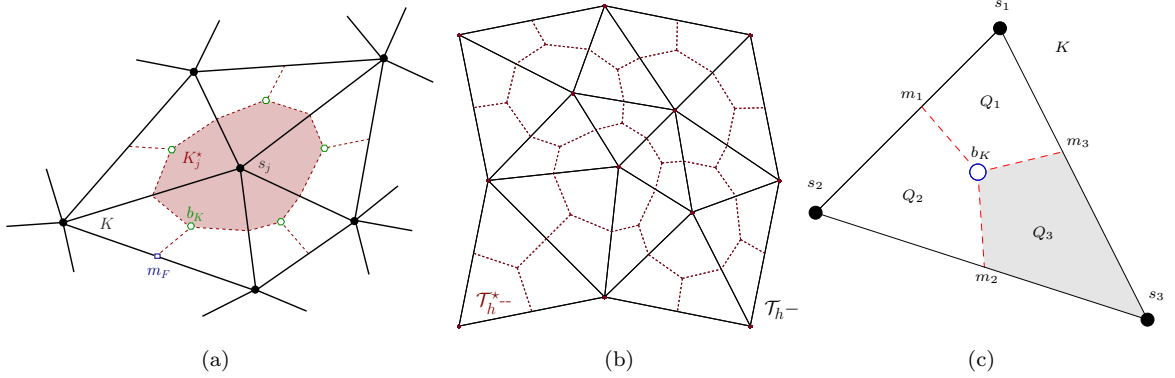


Figure 1: Sketch of five elements in the primal mesh \mathcal{T}_h sharing the vertex s_j and employed to construct the control volume K_j^* belonging to the dual partition \mathcal{T}_h^* (a); example of coarse primal and dual meshes (b); and one triangular element $K \in \mathcal{T}_h$ with barycentre b_K , where the m_i 's denote the midpoints of the edges, and the Q_i 's are the quadrilaterals that form the control volumes (c).

which plays a role in the convergence proof for the envisioned FVE method.

The discrete FVE formulation is obtained by multiplying (2.4) by $\mathbf{v}_h^* \in \mathbf{H}_h^*$ and integrating by parts over each $K_j^* \in \mathcal{T}_h^*$, multiplying (2.5) by $\boldsymbol{\theta}_h \in \mathbf{Z}_h$ and integrating by parts over each $K \in \mathcal{T}_h$, and multiplying (2.6) by $(1 + \eta)q_h$, for $q_h \in \mathbf{Q}_h$, and integrating by parts over each $K \in \mathcal{T}_h$. This, along with identity (1.1), results in a Petrov-Galerkin formulation that reads as follows: Find $((\hat{\boldsymbol{\omega}}_h, \hat{p}_h), \hat{\mathbf{u}}_h) \in (\mathbf{Z}_h \times \mathbf{Q}_h) \times \mathbf{H}_h$ such that

$$a((\hat{\boldsymbol{\omega}}_h, \hat{p}_h), (\boldsymbol{\theta}_h, q_h)) + b((\boldsymbol{\theta}_h, q_h), \hat{\mathbf{u}}_h) = 0 \quad \forall (\boldsymbol{\theta}_h, q_h) \in \mathbf{Z}_h \times \mathbf{Q}_h, \quad (4.2)$$

$$\tilde{b}((\hat{\boldsymbol{\omega}}_h, \hat{p}_h), \mathbf{v}_h^*) = \tilde{F}(\mathbf{v}_h^*) \quad \forall \mathbf{v}_h^* \in \mathbf{H}_h^*, \quad (4.3)$$

where the bilinear form $\tilde{b} : (\mathbf{Z}_h \times \mathbf{Q}_h) \times \mathbf{H}_h^* \rightarrow \mathbb{R}$ and the linear functional $\tilde{F} : \mathbf{H}_h^* \rightarrow \mathbb{R}$ are defined as

$$\begin{aligned} \tilde{b}((\boldsymbol{\theta}_h, q_h), \mathbf{v}_h^*) &:= -(1 + \eta) \sum_{j=1}^{|\mathcal{N}_h|} \int_{\partial K_j^*} q_h (\mathbf{v}_h^* \cdot \mathbf{n}) - \sqrt{\eta} \sum_{j=1}^{|\mathcal{N}_h|} \int_{\partial K_j^*} (\boldsymbol{\theta}_h \times \mathbf{n}) \cdot \mathbf{v}_h^*, \\ \tilde{F}(\mathbf{v}_h^*) &:= - \sum_{j=1}^{|\mathcal{N}_h|} \int_{K_j^*} \mathbf{f} \cdot \mathbf{v}_h^*. \end{aligned}$$

Observe that the bilinear form $\tilde{b}(\cdot, \cdot)$ and the linear functional $\tilde{F}(\cdot)$ are both bounded by positive constants independent of η . We also introduce the bilinear form $B : (\mathbf{Z}_h \times \mathbf{Q}_h) \times \mathbf{H}_h \rightarrow \mathbb{R}$ defined by

$$B((\boldsymbol{\theta}_h, q_h), \mathbf{v}_h) := \tilde{b}((\boldsymbol{\theta}_h, q_h), \mathcal{H}_h \mathbf{v}_h),$$

which allows us to recast the Petrov-Galerkin formulation (4.2)-(4.3) as a standard Galerkin method. If one is interested in imposing mixed boundary conditions (prescribing a displacement \mathbf{g} on $\Gamma_D \subset \partial\Omega$, and setting a given traction \mathbf{t} on the remainder of the boundary), we can modify the FVE scheme as detailed in the Appendix.

We proceed to establish a relationship between the bilinear forms $b(\cdot, \cdot)$ and $B(\cdot, \cdot)$, which will be useful to carry out the error analysis in a finite-element-fashion. For the sake of brevity, only the proof for the two-dimensional case is provided. The proof for the three-dimensional case follows in an analogous manner, where we instead consider polyhedral control volumes and boundary surfaces rather than boundary edges.

Lemma 4.1 For any $(\boldsymbol{\theta}_h, q_h) \in \mathbf{Z}_h \times \mathbf{Q}_h$ and $\mathbf{v}_h \in \mathbf{H}_h$, one has

$$B((\boldsymbol{\theta}_h, q_h), \mathbf{v}_h) := \tilde{b}((\boldsymbol{\theta}_h, q_h), \mathcal{H}_h \mathbf{v}_h) = b((\boldsymbol{\theta}_h, q_h), \mathbf{v}_h). \quad (4.4)$$

Proof. First, let g be a function that is continuous on the interior of each quadrilateral Q_j (as shown in Figure 1(c)) with $\int_e g = 0$ for any boundary edge e . Using Figure 1(c), it is straightforward to show that the following relation holds:

$$\sum_{j=1}^{|\mathcal{N}_h|} \int_{\partial K_j^*} g = \sum_{K \in \mathcal{T}_h} \sum_{j=1}^3 \int_{m_{j+1} b_K m_j} g,$$

where $m_{j+1} b_K m_j$ denotes the union of the line segments $m_{j+1} b_K$ and $b_K m_j$. We take $m_{j+3} = m_j$ in the case that the index is out of bound.

Next, from the definition of the transfer operator $\mathcal{H}_h(\cdot)$, we find that

$$B((\boldsymbol{\theta}_h, q_h), \mathbf{v}_h) = -(1 + \eta) \sum_{j=1}^{|\mathcal{N}_h|} \int_{\partial K_j^*} q_h \mathbf{v}_h(s_j) \cdot \mathbf{n} - \sqrt{\eta} \sum_{j=1}^{|\mathcal{N}_h|} \int_{\partial K_j^*} (\boldsymbol{\theta}_h \times \mathbf{n}) \cdot \mathbf{v}_h(s_j).$$

In order to arrive at (4.4), we use the definition of $B(\cdot, \cdot)$ in combination with integration by parts and the fact that both q_h and $\mathbf{v}_h(s_j)$ are constant in the interior of each quadrilateral Q_j , to obtain

$$\begin{aligned} B((\boldsymbol{\theta}_h, q_h), \mathbf{v}_h) &= -(1 + \eta) \sum_{K \in \mathcal{T}_h} \sum_{j=1}^3 \int_{m_{j+1} b_K m_j} q_h \mathbf{v}_h(s_{j+1}) \cdot \mathbf{n} \\ &\quad - \sqrt{\eta} \sum_{K \in \mathcal{T}_h} \sum_{j=1}^3 \int_{m_{j+1} b_K m_j} (\boldsymbol{\theta}_h \times \mathbf{n}) \cdot \mathbf{v}_h(s_{j+1}) \\ &= (1 + \eta) \sum_{K \in \mathcal{T}_h} \sum_{j=1}^3 q_h \left[\int_{s_j m_j} \mathbf{v}_h(s_{j+1}) \cdot \mathbf{n} + \int_{m_j s_{j+1}} \mathbf{v}_h(s_{j+1}) \cdot \mathbf{n} \right] \\ &\quad + \sqrt{\eta} \sum_{K \in \mathcal{T}_h} \sum_{j=1}^3 \left[\int_{s_j m_j} (\boldsymbol{\theta}_h \times \mathbf{n}) \cdot \mathbf{v}_h(s_{j+1}) + \int_{m_j s_{j+1}} (\boldsymbol{\theta}_h \times \mathbf{n}) \cdot \mathbf{v}_h(s_{j+1}) \right]. \end{aligned}$$

Since q_h and $\boldsymbol{\theta}_h$ are constant on the edges of each element $K \in \mathcal{T}_h$, we can write

$$\begin{aligned} B((\boldsymbol{\theta}_h, q_h), \mathbf{v}_h) &= (1 + \eta) \sum_{K \in \mathcal{T}_h} \sum_{j=1}^3 q_h \int_{s_j s_{j+1}} \mathbf{v}_h \cdot \mathbf{n} + \sqrt{\eta} \sum_{K \in \mathcal{T}_h} \sum_{j=1}^3 \int_{s_j s_{j+1}} (\boldsymbol{\theta}_h \times \mathbf{n}) \cdot \mathbf{v}_h \\ &= (1 + \eta) \sum_{K \in \mathcal{T}_h} \int_{\partial K} q_h \mathbf{v}_h \cdot \mathbf{n} + \sqrt{\eta} \sum_{K \in \mathcal{T}_h} \int_{\partial K} (\boldsymbol{\theta}_h \times \mathbf{n}) \cdot \mathbf{v}_h. \end{aligned}$$

Then, after one application of integration by parts and identity (1.1), we arrive at

$$\begin{aligned} B((\boldsymbol{\theta}_h, q_h), \mathbf{v}_h) &= (1 + \eta) \sum_{K \in \mathcal{T}_h} \int_K q_h \operatorname{div} \mathbf{v}_h - \sqrt{\eta} \sum_{K \in \mathcal{T}_h} \int_K \boldsymbol{\theta}_h \cdot \operatorname{curl} \mathbf{v}_h \\ &= b((\boldsymbol{\theta}_h, q_h), \mathbf{v}_h), \end{aligned}$$

which finishes the proof. \square

Our next goal is to prove a FVE-counterpart of Lemma 3.2, leading to the solvability and stability of (4.2)-(4.3). Recall that Lemma 3.1 establishes that the bilinear form $a(\cdot, \cdot)$ is $(\mathbf{Z}_h \times \mathbf{Q}_h)$ -elliptic, uniformly with respect to the auxiliary parameter η . It is also straightforward to show that the bilinear form $B(\cdot, \cdot)$ satisfies the inf-sup condition, as stated in the following result.

Lemma 4.2 *There exists $C > 0$, independent of η , such that*

$$\sup_{(\boldsymbol{\theta}_h, q_h) \in Z_h \times Q_h} \frac{B((\boldsymbol{\theta}_h, q_h), \mathbf{v}_h)}{\|(\boldsymbol{\theta}_h, q_h)\|_{Z \times Q}} \geq C \|\mathbf{v}_h\|_{\mathbf{H}} \quad \forall \mathbf{v}_h \in \mathbf{H}_h.$$

Proof. This result immediately follows from a straightforward application of Lemma 4.1 in combination with Lemma 3.2. \square

Analogously to the previous section, the following two theorems formulate the unique solvability, stability, best approximation, and convergence properties of the discrete problem (4.2)-(4.3).

Theorem 4.1 *There exists a unique $((\hat{\boldsymbol{\omega}}_h, \hat{p}_h), \hat{\mathbf{u}}_h) \in (Z_h \times Q_h) \times \mathbf{H}_h$ solution of the discrete problem (4.2)-(4.3). Moreover, there exists a constant $C > 0$, independent of h and η , such that*

$$\|(\hat{\boldsymbol{\omega}}_h, \hat{p}_h)\|_{Z \times Q} + \|\hat{\mathbf{u}}_h\|_{\mathbf{H}} \leq C \|\mathbf{f}\|_{0, \Omega}.$$

In addition, the following best approximation result is satisfied

$$\|(\boldsymbol{\omega} - \hat{\boldsymbol{\omega}}_h, p - \hat{p}_h)\|_{Z \times Q} + \|\mathbf{u} - \hat{\mathbf{u}}_h\|_{\mathbf{H}} \leq C \inf_{((\boldsymbol{\theta}_h, q_h), \mathbf{v}_h) \in (Z_h \times Q_h) \times \mathbf{H}_h} \|(\boldsymbol{\omega} - \boldsymbol{\theta}_h, p - q_h)\|_{Z \times Q} + \|\mathbf{u} - \mathbf{v}_h\|_{\mathbf{H}},$$

where $((\boldsymbol{\omega}, p), \mathbf{u}) \in (Z \times Q) \times \mathbf{H}$ is the unique solution of the mixed variational formulation (2.9)-(2.10).

The next lemma establishes linear convergence, which is expected as the only difference with respect to the FE scheme is the right hand side.

Theorem 4.2 *Let $((\boldsymbol{\omega}, p), \mathbf{u}) \in (Z \times Q) \times \mathbf{H}$ and $((\hat{\boldsymbol{\omega}}_h, \hat{p}_h), \hat{\mathbf{u}}_h) \in (Z_h \times Q_h) \times \mathbf{H}_h$ be the solutions of the continuous and discrete problems (2.9)-(2.10) and (4.2)-(4.3), respectively. Then*

$$\|(\boldsymbol{\omega} - \hat{\boldsymbol{\omega}}_h, p - \hat{p}_h)\|_{Z \times Q} + \|\mathbf{u} - \hat{\mathbf{u}}_h\|_{\mathbf{H}} \leq Ch(\|\boldsymbol{\omega}\|_{1, \Omega} + \|p\|_{1, \Omega} + \|\mathbf{u}\|_{2, \Omega}).$$

Proof. Let $((\boldsymbol{\omega}_h, p_h), \mathbf{u}_h)$ and $((\hat{\boldsymbol{\omega}}_h, \hat{p}_h), \hat{\mathbf{u}}_h)$ denote the solutions to the FE formulation (3.1)-(3.2) and the FVE formulation (4.2)-(4.3), respectively. Observe that Lemma 4.1 readily implies that

$$\begin{aligned} a((\boldsymbol{\omega}_h - \hat{\boldsymbol{\omega}}_h, p_h - \hat{p}_h), (\boldsymbol{\theta}_h, q_h)) + b((\boldsymbol{\theta}_h, q_h), \mathbf{u}_h - \hat{\mathbf{u}}_h) &= 0 & \forall (\boldsymbol{\theta}_h, q_h) \in Z_h \times Q_h, \\ b((\boldsymbol{\omega}_h - \hat{\boldsymbol{\omega}}_h, p_h - \hat{p}_h), \mathbf{v}_h) &= F(\mathbf{v}_h - \mathcal{H}_h \mathbf{v}_h) & \forall \mathbf{v}_h \in \mathbf{H}_h, \end{aligned}$$

such that substituting $(\boldsymbol{\omega}_h - \hat{\boldsymbol{\omega}}_h, p_h - \hat{p}_h)$ for $(\boldsymbol{\theta}_h, q_h)$ and $\mathbf{u}_h - \hat{\mathbf{u}}_h$ for \mathbf{v}_h gives

$$a((\boldsymbol{\omega}_h - \hat{\boldsymbol{\omega}}_h, p_h - \hat{p}_h), (\boldsymbol{\omega}_h - \hat{\boldsymbol{\omega}}_h, p_h - \hat{p}_h)) = -b((\boldsymbol{\omega}_h - \hat{\boldsymbol{\omega}}_h, p_h - \hat{p}_h), \mathbf{u}_h - \hat{\mathbf{u}}_h), \quad (4.5)$$

$$b((\boldsymbol{\omega}_h - \hat{\boldsymbol{\omega}}_h, p_h - \hat{p}_h), \mathbf{u}_h - \hat{\mathbf{u}}_h) = F((\mathbf{u}_h - \hat{\mathbf{u}}_h) - \mathcal{H}_h(\tilde{\mathbf{u}}_h - \hat{\mathbf{u}}_h)). \quad (4.6)$$

Next, after applying the inf-sup condition from Lemma 4.2 to equation (4.5), standard arguments imply that there exists a constant $C_0 > 0$, independent of h and η , such that

$$\|\mathbf{u}_h - \hat{\mathbf{u}}_h\|_{\mathbf{H}} \leq C_0 h. \quad (4.7)$$

Moreover, combining equation (4.5) with equation (4.6) relates the bilinear form $a(\cdot, \cdot)$ and the linear functional $F(\cdot)$, such that (4.1) in combination with Lemma 3.1 implies that there exists a constant $C_1 > 0$, independent of h and η , such that

$$\|(\boldsymbol{\omega}_h - \hat{\boldsymbol{\omega}}_h, p_h - \hat{p}_h)\|_{Z \times Q} \leq C_1 h. \quad (4.8)$$

Applying the triangle inequality to the convergence bound for the FE method established in Theorem 3.2 in combination with the inequalities (4.7) and (4.8) finishes the proof. \square

To close this section, we prove an L^2 -estimate for the displacement error. For this purpose we first state a preliminary result (cf. [39]) that involves the transfer operator $\mathcal{H}_h(\cdot)$.

Lemma 4.3 For any function $\mathbf{z}_h \in \mathbf{H}_h$ and any element $K \in \mathcal{T}_h$, one has

$$\int_K (\mathbf{z}_h - \mathcal{H}_h \mathbf{z}_h) = 0.$$

Theorem 4.3 Let $((\boldsymbol{\omega}, p), \mathbf{u}) \in (\mathbf{Z} \times \mathbf{Q}) \times \mathbf{H}$ and $((\hat{\boldsymbol{\omega}}_h, \hat{p}_h), \hat{\mathbf{u}}_h) \in (\mathbf{Z}_h \times \mathbf{Q}_h) \times \mathbf{H}_h$ be the solutions of the continuous and discrete problems (2.9)-(2.10) and (4.2)-(4.3), respectively. Then there exists a constant $C > 0$, independent of h and η , such that

$$\|\mathbf{u} - \hat{\mathbf{u}}_h\|_{0,\Omega} \leq Ch^2 \left[\|\boldsymbol{\omega}\|_{1,\Omega} + \|p\|_{1,\Omega} + \left(\sum_{K \in \mathcal{T}_h} \|\mathbf{f}\|_{1,K}^2 \right)^{1/2} + \|\mathbf{u}\|_{2,\Omega} \right].$$

Proof. Let $((\boldsymbol{\omega}_h, p_h), \mathbf{u}_h)$ and $((\hat{\boldsymbol{\omega}}_h, \hat{p}_h), \hat{\mathbf{u}}_h)$ denote the solutions to the FE formulation (3.1)-(3.2) and the FVE formulation (4.2)-(4.3), respectively. Following the proof of Theorem 3.3, we once again resort to a duality argument involving problem (3.3)-(3.4) with $\hat{\mathbf{u}}_h$ instead of \mathbf{u}_h , for which we assume there exists a unique solution that satisfies the regularity requirement (3.5). Next, we employ identity (3.6) in order to arrive at the envisioned error bound. Using (2.10) and (3.2) in combination with (4.3) and Lemma 4.1, and by adding and subtracting $B((\hat{\boldsymbol{\omega}}_h, \hat{p}_h), \mathbf{z}_h)$ we obtain

$$b((\boldsymbol{\omega} - \hat{\boldsymbol{\omega}}_h, p - \hat{p}_h), \mathbf{z}_h) + b((\hat{\boldsymbol{\omega}}_h - \boldsymbol{\omega}_h, \hat{p}_h - p_h), \mathbf{z}_h) = b((\boldsymbol{\omega}, p), \mathbf{z}_h) - b((\boldsymbol{\omega}_h, p_h), \mathbf{z}_h) = 0, \quad (4.9)$$

such that employing identity (3.7) and identity (4.9) yields

$$\begin{aligned} a((\boldsymbol{\omega} - \hat{\boldsymbol{\omega}}_h, p - \hat{p}_h), (\boldsymbol{\xi}_h, \phi_h)) &= -b((\boldsymbol{\omega} - \hat{\boldsymbol{\omega}}_h, p - \hat{p}_h), \mathbf{z}) - a((\boldsymbol{\omega} - \hat{\boldsymbol{\omega}}_h, p - \hat{p}_h), (\boldsymbol{\xi} - \boldsymbol{\xi}_h, \phi - \phi_h)) \\ &= -b((\boldsymbol{\omega} - \hat{\boldsymbol{\omega}}_h, p - \hat{p}_h), \mathbf{z} - \mathbf{z}_h) - a((\boldsymbol{\omega} - \hat{\boldsymbol{\omega}}_h, p - \hat{p}_h), (\boldsymbol{\xi} - \boldsymbol{\xi}_h, \phi - \phi_h)) \\ &\quad + b((\hat{\boldsymbol{\omega}}_h - \boldsymbol{\omega}_h, \hat{p}_h - p_h), \mathbf{z}_h), \end{aligned} \quad (4.10)$$

which holds for all $\mathbf{z}_h \in \mathbf{H}_h$. In particular, we take the Lagrange interpolant of \mathbf{z} , denoted by $\mathbf{z}_I \in \mathbf{H}_h$. Moreover, for every element $K \in \mathcal{T}_h$, we use $\bar{\mathbf{f}}_K$ to denote the average of \mathbf{f} on such element. Then, by the virtue of Lemma 4.3 and by integrating over elements $K \in \mathcal{T}_h$ instead of over the control volumes $K_j^* \in \mathcal{T}_h^*$ and the domain Ω , we find that for some constant $C_0 > 0$, independent of h and η ,

$$\begin{aligned} |b((\hat{\boldsymbol{\omega}}_h - \boldsymbol{\omega}_h, \hat{p}_h - p_h), \mathbf{z}_I)| &\leq \left| \sum_{j=1}^{|\mathcal{N}_h|} \int_{K_j^*} \mathbf{f} \cdot \mathcal{H}_h \mathbf{z}_I - \int_{\Omega} \mathbf{f} \cdot \mathbf{z}_I \right| \\ &= \left| \sum_{K \in \mathcal{T}_h} \int_K \mathbf{f} \cdot (\mathcal{H}_h \mathbf{z}_I - \mathbf{z}_I) \right| \\ &= \left| \sum_{K \in \mathcal{T}_h} \int_K (\mathbf{f} - \bar{\mathbf{f}}_K) \cdot (\mathcal{H}_h \mathbf{z}_I - \mathbf{z}_I) \right| \\ &\leq C_0 h^2 \left(\sum_{K \in \mathcal{T}_h} \|\mathbf{f}\|_{1,K}^2 \right)^{1/2} |\mathbf{z}_I|_{1,\Omega}, \end{aligned}$$

where the last step follows from the interpolation bound satisfied by the transfer operator $\mathcal{H}_h(\cdot)$. Furthermore, by one application of the triangle inequality it follows that for some constants $C_1, C_2 > 0$, independent of h and η , one has

$$\begin{aligned} |b((\hat{\boldsymbol{\omega}}_h - \boldsymbol{\omega}_h, \hat{p}_h - p_h), \mathbf{z}_I)| &\leq C_0 h^2 \left(\sum_{K \in \mathcal{T}_h} \|\mathbf{f}\|_{1,K}^2 \right)^{1/2} (|\mathbf{z}_I - \mathbf{z}|_{1,\Omega} + |\mathbf{z}|_{1,\Omega}) \\ &\leq C_1 h^2 \left(\sum_{K \in \mathcal{T}_h} \|\mathbf{f}\|_{1,K}^2 \right)^{1/2} (\|\mathbf{z}\|_{2,\Omega} + |\mathbf{z}|_{1,\Omega}) \end{aligned}$$

D.o.f.	h	$e_0(\mathbf{u})$	$r_0(\mathbf{u})$	$e_H(\mathbf{u})$	$r_H(\mathbf{u})$	$e_0(\boldsymbol{\omega})$	$r_0(\boldsymbol{\omega})$	$e_0(p)$	$r_0(p)$
Mixed finite volume element with $k = 1$									
34	0.7071	0.079453	–	0.35510	–	0.04578	–	0.42279	–
68	0.4714	0.063802	0.681	0.27558	0.573	0.04244	0.486	0.36318	0.476
172	0.2828	0.023599	1.540	0.21289	1.021	0.03270	0.638	0.20001	1.034
524	0.1571	0.009612	1.960	0.10311	1.065	0.02033	0.798	0.10700	1.074
1804	0.0831	0.001842	2.071	0.05018	1.073	0.01143	0.921	0.05688	1.079
6668	0.0428	0.000819	2.071	0.02001	1.048	0.00613	0.980	0.02730	1.051
25612	0.0217	0.000079	2.053	0.01295	1.027	0.00304	1.001	0.01258	1.029
100364	0.0109	0.000035	2.027	0.00645	1.015	0.00123	1.002	0.00693	1.016
Mixed finite element with $k = 1$									
34	0.7071	0.082091	–	0.44686	–	0.05045	–	0.44405	–
68	0.4714	0.069138	0.623	0.38582	0.562	0.04647	0.202	0.38301	0.464
172	0.2828	0.033144	1.439	0.22359	1.067	0.03639	0.478	0.22061	1.079
524	0.1571	0.009937	2.049	0.11873	1.076	0.02256	0.813	0.11656	1.085
1804	0.0831	0.002630	2.090	0.06008	1.070	0.01247	0.931	0.05877	1.076
6668	0.0428	0.000661	2.082	0.03000	1.047	0.00649	0.984	0.02929	1.050
25612	0.0217	0.000163	2.062	0.01495	1.027	0.00329	1.002	0.01458	1.028
100364	0.0109	0.000041	2.032	0.00745	1.014	0.00165	1.002	0.00727	1.015
Mixed finite element with $k = 2$									
98	0.7071	0.042104	–	0.19409	–	0.06606	–	0.18250	–
206	0.4714	0.020403	1.788	0.10392	1.549	0.03889	1.903	0.09637	1.577
542	0.2828	0.005284	2.647	0.03914	1.918	0.01338	2.027	0.03678	1.885
1694	0.1571	0.000945	2.923	0.01239	1.956	0.00418	1.973	0.01166	1.956
5918	0.0831	0.000138	3.027	0.00349	1.995	0.00114	2.033	0.00330	1.982
22046	0.0428	0.000018	3.042	0.00092	2.002	0.00029	2.023	0.00087	1.994
85022	0.0217	0.000003	3.018	0.00023	2.002	0.00008	2.052	0.00022	1.992
333854	0.0109	0.000001	3.039	0.00006	2.001	0.00002	2.013	0.00006	1.998

Table 1: Test 1A. Experimental convergence for the mixed Petrov-Galerkin (*cf.* (4.2)-(4.3)) and Galerkin (*cf.* (3.1)-(3.2)) approximation of the compressible linear elasticity equations using $\mu = 50$ and $\lambda = 5000$.

$$\leq C_2 h^2 \left(\sum_{K \in \mathcal{T}_h} \|\mathbf{f}\|_{1,K}^2 \right)^{1/2} \|\mathbf{u} - \hat{\mathbf{u}}_h\|_{0,\Omega}, \quad (4.11)$$

where the last two inequalities follow from the classical error estimates for the Lagrange interpolants and the additional regularity requirement. Hence, by taking the L^2 -projections for ξ and ϕ , using the classical error estimates for the involved spaces, and employing identity (4.10) in combination with inequality (4.11), we straightforwardly deduce that for some constant $C > 0$ (independent of h and η), one has the bound

$$\|\mathbf{u} - \hat{\mathbf{u}}_h\|_{0,\Omega} \leq Ch^2 \left[\|\boldsymbol{\omega}\|_{1,\Omega} + \|p\|_{1,\Omega} + \left(\sum_{K \in \mathcal{T}_h} \|\mathbf{f}\|_{1,K}^2 \right)^{1/2} + \|\mathbf{u}\|_{2,\Omega} \right],$$

thus completing the proof. \square

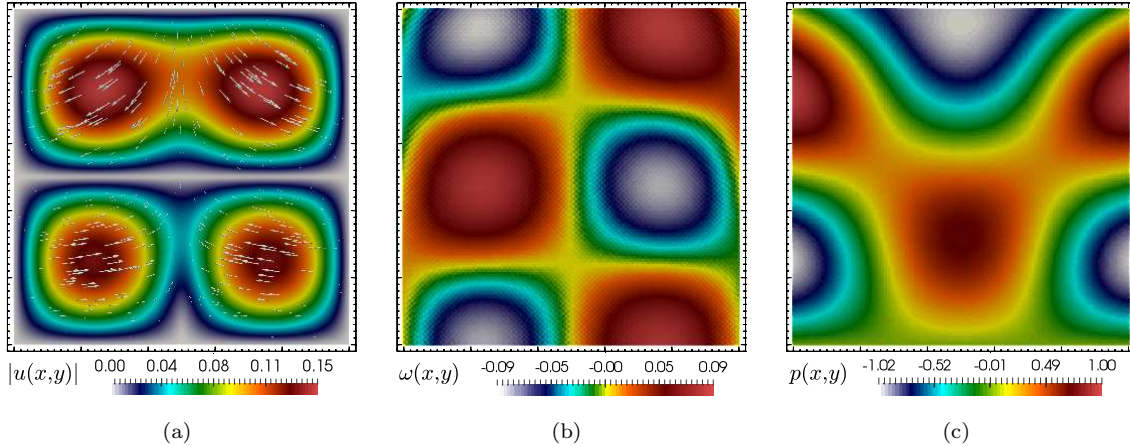


Figure 2: Test 1A (scheme accuracy). Approximate displacement magnitude (a), rotation scalar field (b), and pressure (c); obtained with the lowest order FVE method.

5 Numerical tests

Test 1 (accuracy assessment). For our first computational example we conduct a convergence test using a sequence of successively refined uniform partitions of the elastic domain $\Omega = (0, 1)^2$. We arbitrarily choose the Lamé parameters $\mu = 50$, $\lambda = 5000$, so that $\eta = 0.0099$. This example focuses on the pure-Dirichlet problem (2.4)-(2.7), where we propose the following closed-form solutions

$$\mathbf{u} = \begin{pmatrix} x(1-x)\cos(\pi x)\sin(2\pi y) \\ \sin(\pi x)\cos(\pi y)y^2(1-y) \end{pmatrix}, \quad \boldsymbol{\omega} = \sqrt{\eta} \mathbf{curl} \mathbf{u}, \quad p = -\operatorname{div} \mathbf{u},$$

satisfying the homogeneous Dirichlet datum, and where the forcing term \mathbf{f} is constructed using these smooth functions and the linear momentum equation. The convergence study is performed for the FVE method (4.2)-(4.3) (of lowest order), and for the Galerkin schemes (3.1)-(3.2) of order $k = 1$ and $k = 2$. For a generic scalar or vectorial field \mathbf{v} , on each nested mesh we will denote computed errors and experimental convergence rates as

$$e_0(\mathbf{v}) = \|\mathbf{v} - \mathbf{v}_h\|_{0,\Omega}, \quad e_H(\mathbf{v}) = \|\mathbf{v} - \mathbf{v}_h\|_H, \quad r_i(\mathbf{v}) = \log\left(\frac{e_i(\mathbf{v})}{\widehat{e}(\mathbf{v})}\right) [\log(h/\widehat{h})]^{-1}, \quad i = 0, H,$$

where e, \widehat{e} stand for errors generated by methods defined on meshes with meshsizes h, \widehat{h} , respectively; and we recall that $\|\cdot\|_H$ denotes the η -dependent norm. These errors are tabulated by number of degrees of freedom in Table 1. Apart from the displacement error measured in the L^2 -norm (whose error decays with order h^{k+1} as anticipated by Theorem 3.3), each individual error exhibits an $O(h^k)$ rate of convergence, as expected from the *a priori* error estimates stated in Theorems 3.2 and 4.2. Moreover, the errors produced by the first two methods practically coincide. This is due to the fact that they only differ in the RHS assembly. For reference, in Figure 2 we depict approximate solutions generated with the lowest order FVE scheme. Analogous numerical studies using mixed boundary conditions (see the formulation in the Appendix) produce the same optimal convergence behaviour observed in the pure Dirichlet case.

In addition, these methods are robust with respect to the model parameters, which we confirm by a series of tests where we fix a Young modulus $E = 10000$, we vary the Poisson ratio ν , and measure the errors produced by the first order finite element method on an unstructured mesh of 33282 elements and 100364 D.o.f. (see first block in Table 2). Furthermore, we also construct a different smooth forcing term $\mathbf{f} = (10^5 \cos(x), 10^5 \cos(y))^t$, independent of the model parameters, solve the discrete problem

ν	λ	μ	η	$e_0(\mathbf{u})$	$e_H(\mathbf{u})$	$e_0(\boldsymbol{\omega})$	$e_0(p)$
0.33333	7500	3750.00	0.33333	0.000040	0.01127	0.00807	0.00787
0.40000	14285.71	3571.43	0.20000	0.000038	0.01004	0.00658	0.00758
0.45000	31034.48	3448.28	0.10000	0.000037	0.00886	0.00491	0.00738
0.49000	164429.53	3355.71	0.02000	0.000035	0.00763	0.00232	0.00727
0.49900	1664442.96	3335.56	0.00200	0.000036	0.00730	0.00075	0.00726
0.49990	16664444.30	3333.56	0.00020	0.000039	0.00727	0.00025	0.00726
0.49999	166664444.43	3333.36	0.00002	0.000040	0.00726	0.00008	0.00726
ν	λ	μ	η	$\ \mathbf{u}_h\ _{0,\Omega}$	$\ \mathbf{u}_h\ _H$	$\ \boldsymbol{\omega}_h\ _{0,\Omega}$	$\ p_h\ _{0,\Omega}$
0.33333	7500	3750.00	0.33333	6.346721	23.1147	13.0760	19.0607
0.40000	14285.71	3571.43	0.20000	7.749333	26.3285	12.6964	23.0649
0.45000	31034.48	3448.28	0.10000	9.346012	29.7836	11.1665	27.6111
0.49000	164429.53	3355.71	0.02000	11.28440	33.7542	6.26612	33.1675
0.49900	1664442.96	3335.56	0.00200	11.85713	34.8893	2.10631	34.8257
0.49990	16664444.30	3333.56	0.00020	11.91832	35.0094	0.67041	35.0030
0.49999	166664444.43	3333.36	0.00002	11.92467	35.0215	0.21214	35.0209

Table 2: Test 1B. Accuracy (top rows) and robustness with respect to the Lamé constants (bottom rows) studied on two different benchmark tests approximated with the lowest-order mixed finite element method.

for relatively large Lamé constants (we recall that $\lambda = E\nu/[(1+\nu)(1-2\nu)]$ and $\mu = E/(2+2\nu)$), and tabulate in the bottom block of Table 2 the obtained norms of the approximate solutions. We evidence stable and robust computations even in the regimes of near incompressibility. All linear systems in this example were solved with the Unsymmetric Multi-Frontal sparse LU factorisation (UMFPACK).

Test 2 (2D beam bending). For the next computational example we consider the displacement-rotation-pressure patterns of a rectangular beam (with length $L = 10$ and height $l = 2$) subjected to a *couple* (that is, a prescribed traction $(f(1-y), 0)^\top$, with $f = 200$) at one end, as shown in Figure 3(a). We assume that the origin O is fully fixed and that the horizontal displacement is zero along the left edge of the domain Ω . Furthermore, on the remainder of the boundary we consider zero normal stresses incorporated through the bilinear form $c(\cdot, \cdot)$ (see (A.3)) and we set up a zero body force $\mathbf{f} = \mathbf{0}$. The availability of an exact solution (cf. [30])

$$\mathbf{u}_1(x, y) = \frac{2f(1-\nu)^2}{El}x\left(\frac{l}{2} - y\right), \text{ and } \mathbf{u}_2(x, y) = \frac{f(1-\nu)^2}{El}\left[x^2 + \frac{\nu}{1+\nu}y(y-l)\right], \quad (5.1)$$

makes that this problem is frequently used as a benchmark. In Figure 3 we illustrate the components of the displacement, the rotation and the pressure computed on a mesh consisting of 5120 triangular elements using the mixed FE method corresponding to $k = 2$, where the rectangular beam we consider has the following material properties: Young's modulus $E = 1500$, Poisson's ratio $\nu = 0.49$, Lamé constants $\lambda = 24664.4$ and $\mu = 503.356$, such that the model parameter equals $\eta = 0.02$. In addition, we conduct several tests for the lowest order mixed FE and FVE methods on different mesh resolutions and report on the error with respect to the analytic solution (5.1). In particular, Figure 4 displays the displacement error in the H-norm and the L²-norm versus the meshsize, for the FE and FVE schemes, and for two values of the Poisson ratio $\nu = 0.49, 0.4999$. The Young's modulus is in both cases $E = 1500$. Observe that these results are in agreement with the theoretical results obtained in Sections 3-4. In addition, although this is in general not true, we mention that the second order FE scheme ensures extremely rapid convergence (explained by the regularity of the true solution (5.1)). For $\nu = 0.4999$, optimal convergence is recovered for finer meshes.

We also perform a series of tests for the lowest order FE method using different Lamé constants

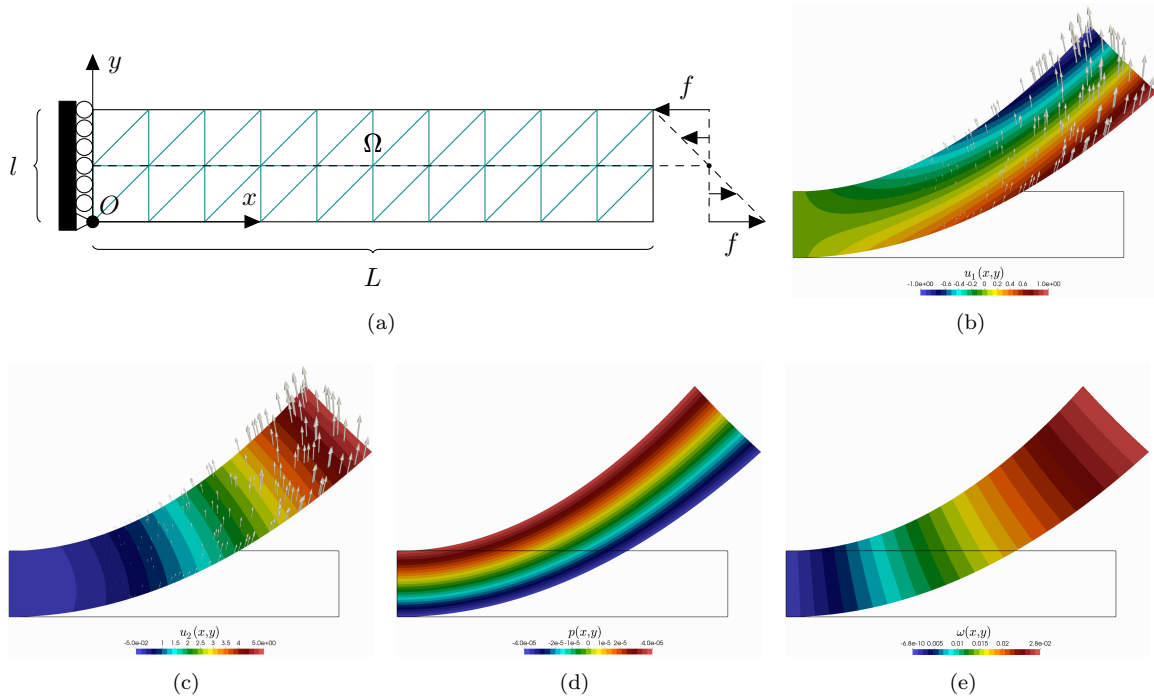


Figure 3: Test 2. Rectangular beam fixed at the origin O and with zero horizontal displacement along the left lateral edge, subjected to bending due to a couple at one end. Sketch of the domain configuration with a coarse structured mesh and the imposed boundary conditions (a), displacement components (b,c), pressure distribution (d), and rotation (e); all computed with a second order mixed FE method on a mesh of 5120 triangular elements.

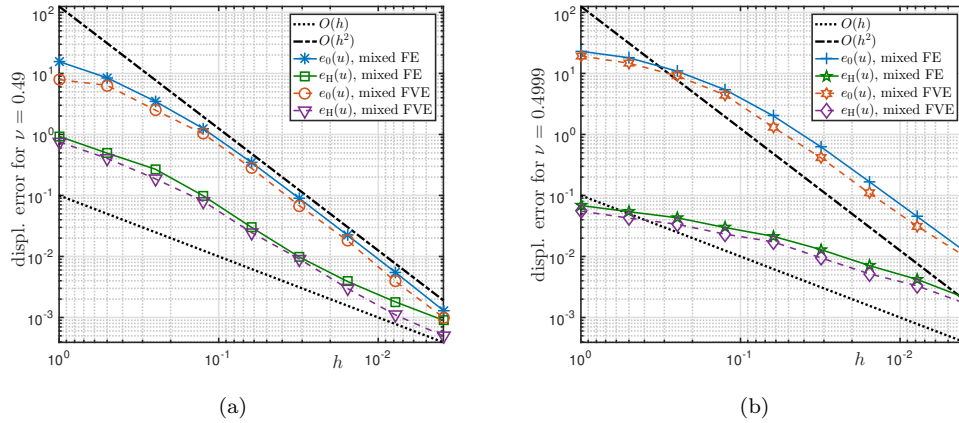


Figure 4: Test 2. Convergence history for the displacement approximation using the first order mixed FE and FVE schemes, for $\nu = 0.49$ (a) and $\nu = 0.4999$ (b).

and model parameters in order to test the performance of the methods when approaching the incompressibility limit, where we fix a Young's modulus $E = 1500$, vary the Poisson ratio ν , and use a mesh consisting of 100000 triangular elements and using 301201 D.o.f.. Based on the comparisons in Table 3, we observe that the performance is barely modified for large values of λ .

ν	λ	μ	η	$e_0(\mathbf{u})$	$e_H(\mathbf{u})$	$\ \mathbf{u}_h\ _{0,\Omega}$	$\ \mathbf{u}_h\ _H$
0.2000	416.667	625.00	0.6000	0.0041	0.0048	12.9021	0.9667
0.3333	1124.69	562.51	0.3333	0.0044	0.0046	11.9137	0.8786
0.4000	2142.86	535.71	0.2000	0.0055	0.0045	11.2365	0.8231
0.4500	4655.17	517.24	0.1000	0.0088	0.0045	10.6469	0.7774
0.4900	24664.4	503.36	0.0200	0.0367	0.0053	10.1009	0.7371
0.4990	249666	500.33	0.0020	0.3426	0.0269	9.6729	0.7047
0.4999	2499666	500.03	0.0002	2.5086	0.1928	7.4972	0.5378

Table 3: Test 2. Displacement errors for different Lamé constants produced by the lowest order mixed FE method on an regular mesh of 100000 triangular elements, for a fixed Young’s modulus $E = 1500$.

$k \backslash h$	$(w/4)^3$	$(w/8)^3$	$(w/16)^3$	$(w/32)^3$	$(w/64)^3$
1	-0.4322	-0.4465	-0.4688	-0.4691	-0.4695
2	-0.4671	-0.4694	-0.4702	-0.4703	-0.4704
3	-0.4693	-0.4701	-0.4704	-0.4704	-0.4704

Table 4: Test 3. Maximal deflection of a beam computed at the point $(x_0, y_0, z_0) = (\ell, \frac{1}{2}w, \frac{1}{2}w)$, according to meshsize and discretisation order. The expected value corresponds to $\delta = -0.47040$.

Test 3 (3D beam bending). We also consider a three-dimensional beam problem. The beam occupies the domain $\Omega = (0, \ell) \times (0, w) \times (0, w)$, with $\ell = 2.5$, $w = 0.5$ (see a sketch in Figure 5(a)); and its elastic properties are characterised by a Young modulus of $E = 1000$ and a Poisson ratio $\nu = 0.3$, giving Lamé constants $\lambda = 576.923$, $\mu = 384.615$, and the coefficient $\eta = 0.4$. The body force acts in the direction of gravity $\tilde{\mathbf{f}} = (0, 0, -\rho g)^\top$ and it is specified by $g = 9.8$ and $\rho = 0.2$. Zero displacements are enforced on the face $x = 0$, whereas on the remainder of the boundary we consider zero normal stresses incorporated through the term $\int_{x>0} 2\eta(\nabla \mathbf{u} - \text{div } \mathbf{u} \mathbf{I}) \mathbf{n} \cdot \mathbf{v}$ defining the bilinear form $c(\cdot, \cdot)$ (see (A.3)). In Figure 5 we illustrate (on the deformed configuration) the displacement, rotation vector, and pressure computed on a mesh of 45221 tetrahedral elements, employing a method of order $k = 2$. In the case of gravity-induced deflection, the Euler-Bernoulli beam theory predicts a maximum vertical deflection of $\delta = \rho g A \ell / (8EI)$, occurring at the free end of the body, $A = w^2$ is the area of the cross-section, and $I = A^4/12$ is the planar inertial moment. Table 4 compares the expected deflection with the vertical displacement measured on the midpoint of the face located at $x = \ell$, for different discretisation choices.

Test 4 (Cook’s membrane benchmark). We finalise the set of tests by considering a two-dimensional quadrilateral panel with domain Ω defined as the convex hull of the set $\{(0, 0), (\ell, w), (\ell, \ell + s), (0, w)\}$, with $\ell = 48$, $w = 44$, $s = 16$, and proceed to study its elastic response dominated by bending and shear. This benchmark is known as Cook’s membrane problem (*cf.* [14]). The panel is clamped at the left edge ($x = 0$) and the body is subjected to a shearing distributed load $\tilde{\mathbf{t}} = (0, 1/s)^\top$ on the opposite end (at $x = \ell$ and giving a resulting load of magnitude 1, see a sketch in Figure 6(a)). This effect is incorporated in the formulation through the term $-\int_{x=\ell} \tilde{\mathbf{t}} \cdot \mathbf{v} \, ds$ added to the functional $F(\cdot)$ in the modified weak formulation (A.1)-(A.2). A traction-free condition is applied on the non-vertical boundaries (imposed as in the previous test, using (A.3)), and we set up a zero volume force $\tilde{\mathbf{f}} = \mathbf{0}$ (so that the weight of the membrane is not considered). The elastic plate has Young’s modulus $E = 1$, Poisson ratio $\nu = 1/3$, Lamé constants $\lambda = 3/4$, $\mu = 3/8$, and model coefficient $\eta = 1/3$. Figure 6 portrays the displacement, rotation and pressure fields on the deformed domain (without amplification of the deformation field). We also conduct several tests for different mesh resolutions and report on the vertical displacement (deflection) measured at the midpoint of the right end of the domain,

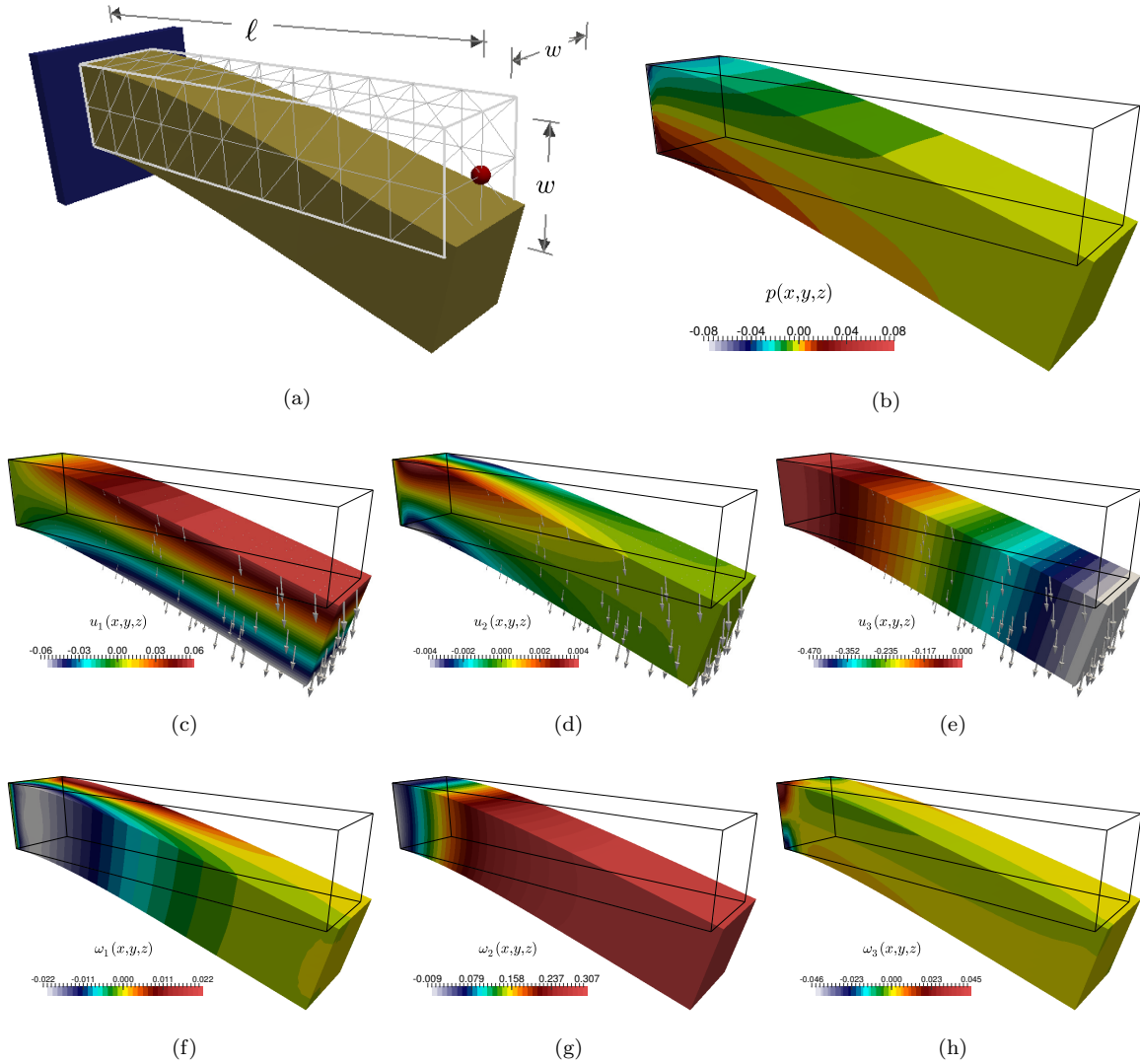


Figure 5: Test 3. Cantilever beam fixed on the left end and subjected to bending due to distributed load applied in the gravity direction. Sketch of the domain configuration and a coarse structured mesh (a), pressure distribution (b), displacement components (c,d,e), and rotation vector components (f,g,h); all computed with a second order finite element method.

$(x_0, y_0) = (\ell, \ell + s/2)$. The test results are shown in panel (b) of the figure, where the convergence behaviour of the deflection is observed as a function of the number of points discretising the right edge of the membrane. In the absence of a known closed form solution for this problem, we also include a referential value reported in the literature (according to [18, 29, 35], under plane stress conditions the maximum vertical displacement expected at this point is around 23.92).

To conclude we perform again the Cook's membrane test, but focusing in the nearly incompressibility limit. We choose the model parameters $E = 250$, $\nu = 0.4999$, $\lambda = 416611$, $\mu = 83.3389$, and $\eta = 0.0002$. As reference value for the maximum deflection at the point (x_0, y_0) we consider 7.505 (see [32, 37, 42]), and conduct a convergence analysis portrayed in Figure 6(c). This time the vertical displacement is plotted against the D.o.f. associated to the underlying discretisation, where we also include a comparison against numerical results obtained with other finite element formulations applied

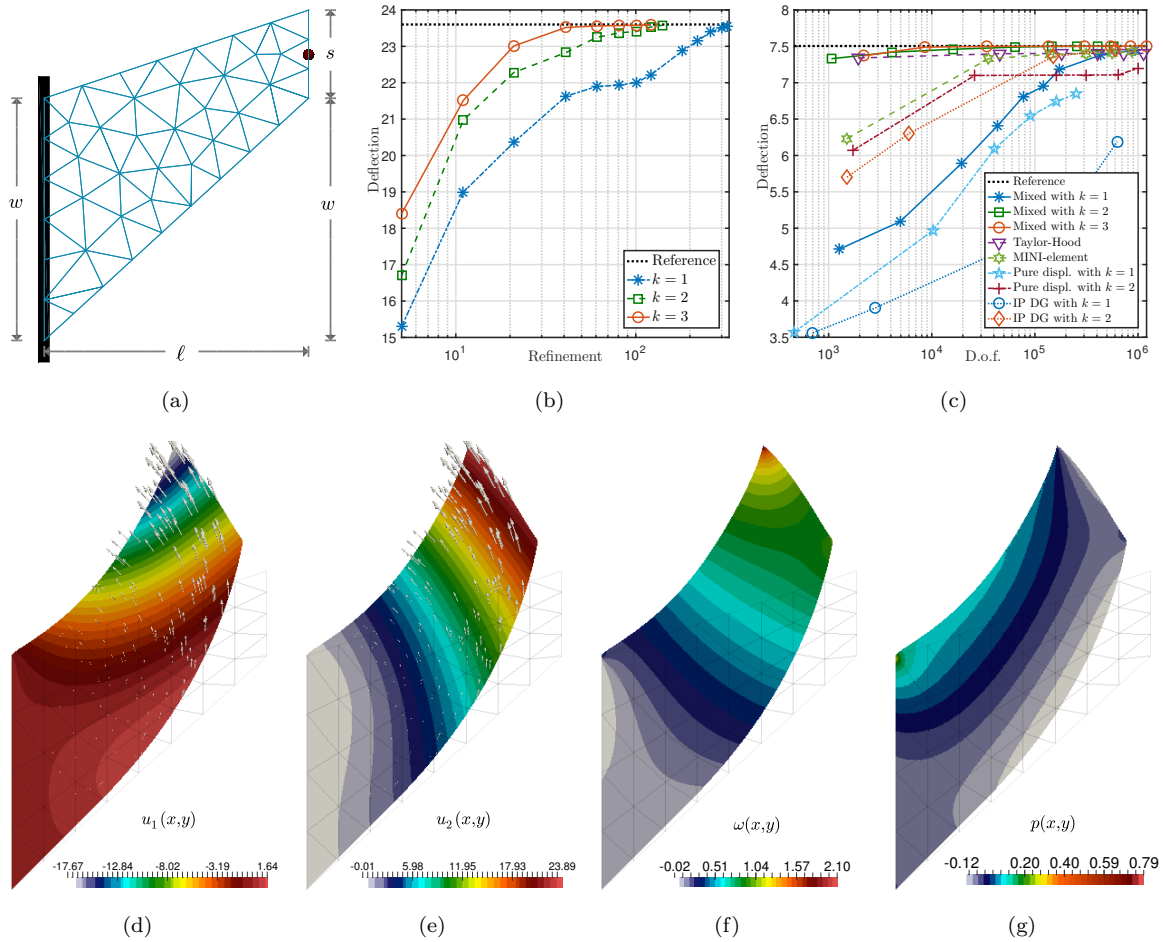


Figure 6: Test 4. Cook's membrane test where the left edge is clamped and an upward shear force is applied on the right edge. Sketch of the domain configuration and a coarse structured mesh (a), maximum deflection of the right edge midpoint according to spatial resolution and approximation order, using $\nu = 0.3$ (b), and according to the number of degrees of freedom and comparison against other classical methods, using $\nu = 0.4999$ (c), approximate displacement components (d,e), rotation scalar (f), and pressure (g); all computed with a second order mixed method.

to the original equations (2.1) (a classical pure-displacement formulation discretised with piecewise continuous elements of degree k , the Taylor-Hood finite element for a displacement-pressure formulation, the MINI-element [2], and a stabilised interior-penalty DG method [5]). These schemes have comparable complexity, and we do not include other mixed methods based on stress or pseudo-stress formulations, (as their associated cost would be much higher). In any case, we highlight the competitive performance of the methods proposed in this paper (in particular for $k = 2$ and $k = 3$), and envisage many extensions including formulations in finite elasticity and coupled elasticity-diffusion problems.

Acknowledgments. This work has been partially supported by CONICYT-Chile through the FONDECYT projects 11160706 and 1140791; by DIUBB through project 165608-3/R; and by the EPSRC through the Research Grant EP/R00207X/1.

A Appendix. The case of mixed boundary conditions

Let us consider the Cauchy-Navier equations, now furnished with the mixed boundary conditions (2.8). Testing (2.4) against $\mathbf{v} \in \tilde{\mathbf{H}} := \mathbf{H}_{\Gamma_D}^1(\Omega)^d = \{\mathbf{v} \in \mathbf{H}^1(\Omega)^d : \mathbf{v}|_{\Gamma_D} = \mathbf{0}\}$, and integrating by parts using (1.1), leads to

$$-(1+\eta) \int_{\Omega} p \operatorname{div} \mathbf{v} + (1+\eta) \int_{\Gamma_N} \mathbf{v} \cdot (p\mathbf{n}) + \sqrt{\eta} \int_{\Omega} \boldsymbol{\omega} \cdot \operatorname{curl} \mathbf{v} + \sqrt{\eta} \int_{\Gamma_N} (\boldsymbol{\omega} \times \mathbf{n}) \cdot \mathbf{v} = \int_{\Omega} \mathbf{f} \cdot \mathbf{v} \quad \forall \mathbf{v} \in \tilde{\mathbf{H}}.$$

We then use the definition of the traction \mathbf{t} (second relation in (2.8)) to obtain

$$-(1+\eta) \int_{\Omega} p \operatorname{div} \mathbf{v} + (1+\eta) \int_{\Gamma_N} \mathbf{v} \cdot (p\mathbf{n}) + \sqrt{\eta} \int_{\Omega} \boldsymbol{\omega} \cdot \operatorname{curl} \mathbf{v} + \int_{\Gamma_N} [2\eta(\nabla \mathbf{u})\mathbf{n} - (1-\eta)p\mathbf{n} - \mathbf{t}] \cdot \mathbf{v} = \int_{\Omega} \mathbf{f} \cdot \mathbf{v},$$

for all $\mathbf{v} \in \tilde{\mathbf{H}}$.

Therefore, employing equation (2.6) and rearranging terms, we arrive at the following modification of (2.9)-(2.10) incorporating mixed displacement-traction boundary conditions: Find $((\boldsymbol{\omega}, p), \mathbf{u}) \in (\mathbf{Z} \times \mathbf{Q}) \times \tilde{\mathbf{H}}$ such that

$$a((\boldsymbol{\omega}, p), (\boldsymbol{\theta}, q)) + b((\boldsymbol{\theta}, q), \mathbf{u}) = 0 \quad \forall (\boldsymbol{\theta}, q) \in \mathbf{Z} \times \mathbf{Q}, \quad (\text{A.1})$$

$$b((\boldsymbol{\omega}, p), \mathbf{v}) - c(\mathbf{u}, \mathbf{v}) = F(\mathbf{v}) - \int_{\Gamma_N} \mathbf{t} \cdot \mathbf{v} \quad \forall \mathbf{v} \in \tilde{\mathbf{H}}, \quad (\text{A.2})$$

where the additional diagonal bilinear form $c : \tilde{\mathbf{H}} \times \tilde{\mathbf{H}} \rightarrow \mathbb{R}$ is defined as

$$c(\mathbf{u}, \mathbf{v}) := 2\eta \int_{\Gamma_N} [\nabla \mathbf{u} - (\operatorname{div} \mathbf{u})\mathbf{I}]\mathbf{n} \cdot \mathbf{v}, \quad \forall \mathbf{u}, \mathbf{v} \in \tilde{\mathbf{H}}. \quad (\text{A.3})$$

Note that since $\mathbf{u} \in \tilde{\mathbf{H}}$ and $\operatorname{div}(2\mu\boldsymbol{\varepsilon}(\mathbf{u}) + \lambda \operatorname{div} \mathbf{u})$ is in $L^2(\Omega)^d$, then $2\eta(\nabla \mathbf{u}\mathbf{n} - \operatorname{div} \mathbf{u}\mathbf{n})$ is in $H^{-1/2}(\Gamma_N)^d$. Therefore the bilinear form $c(\cdot, \cdot)$ is simply a duality pairing between $H^{-1/2}$ and $H^{1/2}$. A similar observation can be found in [3].

The Galerkin formulation will then adopt an analogous structure. In turn, the FVE method from Section 4 can be modified to incorporate mixed boundary conditions as follows. We consider the discrete space

$$\tilde{\mathbf{H}}_h^* := \{\mathbf{v} \in L^2(\Omega)^d : \mathbf{v}|_{K_j^*} \in \mathcal{P}_0(K_j^*)^d \text{ for all } K_j^* \in \mathcal{T}_h^*, \mathbf{v}|_{K_j^*} = \mathbf{0} \text{ if } s_j \in K_j^* \text{ lies on } \Gamma_D\}.$$

In view of discretising the Cauchy-Navier equations subject to mixed boundary conditions (2.8), we can test (2.4) against $\mathbf{v}_h^* \in \tilde{\mathbf{H}}_h^*$ and integrate by parts, which leads to

$$(1+\eta) \sum_{j=1}^{|\mathcal{N}_h|} \int_{\partial K_j^*} p_h \mathbf{v}_h^* \cdot \mathbf{n} + \sqrt{\eta} \sum_{j=1}^{|\mathcal{N}_h|} \int_{\partial K_j^*} (\boldsymbol{\omega}_h \times \mathbf{n}) \cdot \mathbf{v}_h^* = \sum_{j=1}^{|\mathcal{N}_h|} \int_{K_j^*} \mathbf{f} \cdot \mathbf{v}_h^* \quad \forall \mathbf{v}_h^* \in \tilde{\mathbf{H}}_h^*.$$

Next, we employ an argument similar to the one used in the proof of Lemma 4.1 by considering the edges that coincide with the boundary segment Γ_N separately. More precisely, by substituting $\mathcal{H}_h \mathbf{v}_h$ and by definition of the traction \mathbf{t} , we readily obtain

$$(1+\eta) \left[\sum_{K \in \mathcal{T}_h} \int_{\partial K / \Gamma_N} p_h \mathbf{v}_h \cdot \mathbf{n} + \sum_{j=1}^{|\mathcal{N}_h|} \int_{\partial K_j^* \cap \Gamma_N} p_h \mathcal{H}_h \mathbf{v}_h \cdot \mathbf{n} \right] \\ + \sqrt{\eta} \left[\sum_{K \in \mathcal{T}_h} \int_{\partial K / \Gamma_N} (\boldsymbol{\omega}_h \times \mathbf{n}) \cdot \mathbf{v}_h + \sum_{j=1}^{|\mathcal{N}_h|} \int_{\partial K_j^* \cap \Gamma_N} (\boldsymbol{\omega}_h \times \mathbf{n}) \cdot \mathcal{H}_h \mathbf{v}_h \right]$$

$$+ \sum_{j=1}^{|\mathcal{N}_h|} \int_{\partial K_j^* \cap \Gamma_N} [2\eta(\nabla \mathbf{u}_h) \mathbf{n} - (1-\eta)p_h \mathbf{n} - \mathbf{t}] \cdot \mathcal{H}_h \mathbf{v}_h = \sum_{j=1}^{|\mathcal{N}_h|} \int_{K_j^*} \mathbf{f} \cdot \mathcal{H}_h \mathbf{v}_h,$$

for all $\mathbf{v}_h \in \tilde{\mathbb{H}}_h$. In order to simplify the previous expression further, we use that $\int_e (\mathcal{H}_h \mathbf{v}_h - \mathbf{v}_h) = 0$ for every $\mathbf{v}_h \in \tilde{\mathbb{H}}_h$ and every edge e of each element $K \in \mathcal{T}_h$ (cf. [39]) in combination with the assumption that $p_h \in \mathbb{Q}_h$ and $\boldsymbol{\omega}_h \in \mathbb{Z}_h$ are both constant on each element $K \in \mathcal{T}_h$, which implies that

$$\sum_{j=1}^{|\mathcal{N}_h|} \int_{\partial K_j^* \cap \Gamma_N} p_h \mathcal{H}_h \mathbf{v}_h \cdot \mathbf{n} = \sum_{K \in \mathcal{T}_h} \int_{\partial K \cap \Gamma_N} p_h \mathcal{H}_h \mathbf{v}_h \cdot \mathbf{n} = \sum_{K \in \mathcal{T}_h} \int_{\partial K \cap \Gamma_N} p_h \mathbf{v}_h \cdot \mathbf{n}, \quad (\text{A.4})$$

$$\sum_{j=1}^{|\mathcal{N}_h|} \int_{\partial K_j^* \cap \Gamma_N} (\boldsymbol{\omega}_h \times \mathbf{n}) \cdot \mathcal{H}_h \mathbf{v}_h = \sum_{K \in \mathcal{T}_h} \int_{\partial K \cap \Gamma_N} (\boldsymbol{\omega}_h \times \mathbf{n}) \cdot \mathcal{H}_h \mathbf{v}_h = \sum_{K \in \mathcal{T}_h} \int_{\partial K \cap \Gamma_N} (\boldsymbol{\omega}_h \times \mathbf{n}) \cdot \mathbf{v}_h, \quad (\text{A.5})$$

where we have also used that the union of boundary edges of control volumes and the union of boundary edges of elements coincide. Consequently, after joining integrals by employing (A.4)-(A.5) and using identity (1.1), we obtain the following modification of the FVE formulation when incorporating mixed displacement-traction boundary conditions: Find $((\hat{\boldsymbol{\omega}}_h, \hat{p}_h), \hat{\mathbf{u}}_h) \in (\mathbb{Z}_h \times \mathbb{Q}_h) \times \tilde{\mathbb{H}}_h$ such that

$$\begin{aligned} a((\hat{\boldsymbol{\omega}}_h, \hat{p}_h), (\boldsymbol{\theta}_h, q_h)) + b((\boldsymbol{\theta}_h, q_h), \hat{\mathbf{u}}_h) &= 0 & \forall (\boldsymbol{\theta}_h, q_h) \in \mathbb{Z}_h \times \mathbb{Q}_h, \\ b((\hat{\boldsymbol{\omega}}_h, \hat{p}_h), \mathbf{v}_h) - C(\hat{\mathbf{u}}_h, \mathbf{v}_h) &= \tilde{F}(\mathbf{v}_h) - \sum_{j=1}^{|\mathcal{N}_h|} \int_{\partial K_j^* \cap \Gamma_N} \mathbf{t} \cdot \mathcal{H}_h \mathbf{v}_h & \forall \mathbf{v}_h \in \tilde{\mathbb{H}}_h, \end{aligned}$$

where the newly introduced bilinear form $C : \tilde{\mathbb{H}}_h \times \tilde{\mathbb{H}}_h \rightarrow \mathbb{R}$ is defined as

$$C(\mathbf{u}_h, \mathbf{v}_h) := 2\eta \sum_{j=1}^{|\mathcal{N}_h|} \int_{\partial K_j^* \cap \Gamma_N} [\nabla \mathbf{u}_h - (\operatorname{div} \mathbf{u}_h) \mathbf{I}] \mathbf{n} \cdot \mathcal{H}_h \mathbf{v}_h, \quad \forall \mathbf{u}_h, \mathbf{v}_h \in \tilde{\mathbb{H}}_h. \quad (\text{A.6})$$

Moreover, using a similar argument as before in combination with the assumption that $\mathbf{u}_h \in \tilde{\mathbb{H}}_h$ is linear on each element $K \in \mathcal{T}_h$, we find that

$$C(\mathbf{u}_h, \mathbf{v}_h) - c(\mathbf{u}_h, \mathbf{v}_h) = 2\eta \sum_{K \in \mathcal{T}_h} \int_{\partial K \cap \Gamma_N} [\nabla \mathbf{u}_h - (\operatorname{div} \mathbf{u}_h) \mathbf{I}] \mathbf{n} \cdot (\mathcal{H}_h \mathbf{v}_h - \mathbf{v}_h) = 0,$$

for all $\mathbf{u}_h, \mathbf{v}_h \in \tilde{\mathbb{H}}_h$. In other words, also for mixed displacement-traction boundary conditions we find that the lowest order FE and FVE schemes only differ by assembly of the right hand side.

References

- [1] U. ANDEFINGER AND E. RAMM, *EAS-elements for two-dimensional, three-dimensional, plate and shell structures and their equivalence to HR-elements*. Int. J. Numer. Methods Engrg., 36(8) (1993) 1311–1337.
- [2] D.N. ARNOLD, F. BREZZI, AND M. FORTIN, *A stable finite element for the Stokes equations*. Calcolo, 21 (1984) 337–344.
- [3] D.N. ARNOLD AND R.S. FALK, *A new mixed formulation for elasticity*. Numer. Math., 53(1-2) (1988) 13–30.
- [4] D.N. ARNOLD, R.S. FALK, AND R. WINTHER, *Mixed finite element methods for linear elasticity with weakly imposed symmetry*. Math. Comp., 76 (2007) 1699–1723.
- [5] D. BAROLI, A. QUARTERONI, AND R. RUIZ-BAIER, *Convergence of a stabilized discontinuous Galerkin method for incompressible nonlinear elasticity*. Adv. Comput. Math., 39 (2013) 425–443.

- [6] L. BEIRÃO DA VEIGA, D. MORA, AND R. RODRÍGUEZ, *Numerical analysis of a locking-free mixed finite element method for a bending moment formulation of Reissner-Mindlin plate model*. Numer. Methods Partial Diff. Eqns., 29 (2013) 40–63.
- [7] E. BERTÓTI, *Dual-mixed hp finite element methods using first-order stress functions and rotations*. Comput. Mech., 26 (2000) 39–51.
- [8] D. BOFFI, F. BREZZI, AND M. FORTIN, *Reduced symmetry elements in linear elasticity*. Commun. Pure Appl. Anal., 8(1) (2009) 95–121.
- [9] D. BRAESS, *Finite Elements. Theory, Fast Solvers, and Applications in Solid Mechanics*, 2nd Ed., Cambridge University Press, Cambridge, 2001.
- [10] D. BRAESS, C. CARSTENSEN, AND B. D. REDDY, *Uniform convergence and a posteriori error estimators for the enhanced strain finite element method*. Numer. Math., 96(3) (2004) 461–479.
- [11] F. BREZZI AND M. FORTIN, *Mixed and Hybrid Finite Element Methods*. Springer-Verlag, New York, 1991.
- [12] Z. CAI, T. MANTEUFFEL, AND S. MCCORMICK, *First-order system least squares for the Stokes equations, with application to linear elasticity*. SIAM J. Numer. Anal., 34(5) (1997) 1727–1741.
- [13] C. CARSTENSEN, N. NATARAJ, AND A.K. PANI, *Comparison results and unified analysis for first-order finite volume element methods for a Poisson model problem*. IMA J. Numer. Anal., 36(3) (2016) 1120–1142.
- [14] R.D. COOK, *Improved two-dimensional finite element*. ASCE J. Struct. Div., ST9 (1974) 1851–1863.
- [15] J.K. DJOKO, B.P. LAMICHHANE, B.D. REDDY, AND B.I. WOHLMUTH, *Conditions for equivalence between the Hu-Washizu and related formulations and computational behavior in the incompressible limit*. Comput. Methods Appl. Mech. Engrg., 195(33-36) (2006) 4161–4178.
- [16] R.E. EWING, R.D. LAZAROV, AND Y. LIN, *Finite volume element approximations of nonlocal reactive flows in porous media*. Numer. Methods Partial Diff. Eqns., 16 (2000) 285–311.
- [17] M. FEISTAUER, J. FELCMAN, AND M. LUKÁČOVÁ-MEDVID’OVÁ, *Combined finite element-finite volume solution of compressible flow*. J. Comput. Appl. Math., 63 (1995) 179–199.
- [18] M. FREDRIKSSON AND N.S. OTTOSEN, *Fast and accurate 4-node quadrilateral*. Int. J. Numer. Methods Engrg., 61 (2004) 1809–1834.
- [19] G.N. GATICA, *A Simple Introduction to the Mixed Finite Element Method. Theory and Applications*. Springer Briefs in Mathematics, Springer, Cham Heidelberg New York Dordrecht London, (2014).
- [20] G.N. GATICA, *Analysis of a new augmented mixed finite element method for linear elasticity allowing $\mathbb{RT}_0 - \mathbb{P}_1 - \mathbb{P}_0$ approximations*. ESAIM Math. Model. Numer. Anal., 40(1) (2006) 1–28.
- [21] G.N. GATICA, L.F. GATICA, AND F. SEQUEIRA, *A priori and a posteriori error analyses of a pseudostress-based formulation for linear elasticity*. Comput. Math. Appl., 71 (2016) 585–614.
- [22] G.N. GATICA, A. MÁRQUEZ, AND S. MEDDAHI, *An augmented mixed finite element method for 3D linear elasticity problems*. J. Comput. Appl. Math., 231 (2009) 526–540.
- [23] V. GIRAULT, AND P. A. RAVIART, *Finite Element Methods for Navier-Stokes Equations. Theory and algorithms*. Springer-Verlag, Berlin, 1986.
- [24] G. HE, Y. HE, AND X. FENG, *Finite volume method based on stabilized finite elements for the nonstationary Navier-Stokes problem*. Numer. Methods Part. Diff. Eqns., 23 (2007) 1167–1191.
- [25] H. HU, *On some variational principles in the theory of elasticity and the theory of plasticity*. Acta Phys. Sin., 10(3) (1954) 259–290.
- [26] T.J.R. HUGHES, *The Finite Element Method: Linear Static and Dynamic Finite Element Analysis*. Prentice-Hall, New Jersey, 1987.

- [27] T.J.R. HUGHES, A. MASUD, AND I. HARARI, *Numerical assessment of some membrane elements with drilling degrees of freedom*. *Comput. Struct.*, 55(2) (1995) 297–314.
- [28] E.P. KASPER AND R.L. TAYLOR, *A mixed-enhanced strain method, Part I: geometrically linear problems*. *Comput. Struct.*, 75(3) (2000) 237–250.
- [29] Y. KO, P.S. LEE, AND K.J. BATHE, *The MITC4+ shell element and its performance*. *Comput. Struct.*, 169 (2016) 57–68.
- [30] B.P. LAMICHHANE, *Higher Order Mortar Finite Elements with Dual Lagrange Multiplier Spaces and Applications*. Ph.D Thesis Universität Stuttgart, Stuttgart, 2006.
- [31] B.P. LAMICHHANE, *Inf-sup stable finite-element pairs based on dual meshes and bases for nearly incompressible elasticity*. *IMA J. Numer. Anal.*, 29 (2009) 404–420.
- [32] B.P. LAMICHHANE, A.T. MCBRIDE, AND B.D. REDDY, *A finite element method for a three-field formulation of linear elasticity based on biorthogonal systems*. *Comput. Methods Appl. Mech. Engrg.*, 258 (2013) 109–117.
- [33] B.P. LAMICHHANE, B.D. REDDY, AND B.I. WOHLMUTH, *Convergence in the incompressible limit of finite element approximations based on the Hu-Washizu formulation*. *Numer. Math.*, 104(2) (2006) 151–175.
- [34] J. LI AND Z. CHEN, *A new stabilized finite volume method for the stationary Stokes equations*. *Adv. Comput. Math.*, 30 (2009) 141–152.
- [35] G.R. LIU, T. NGUYEN-THOI, AND K.Y. LAM, *A novel alpha finite element method (α FEM) for exact solution to mechanics problems using triangular and tetrahedral elements*. *Comput. Methods Appl. Mech. Engrg.*, 197 (2008) 3883–3897.
- [36] Z. LUO AND F. TENG, *A fully discrete SCNFVE formulation for the non-stationary Navier-Stokes equations*. *Comput. Model. Eng. Sci.*, 101 (2014) 33–58.
- [37] K.B. NAKSHATRALA, A. MASUD, AND K.D. HJELMSTAD, *On finite element formulations for nearly incompressible linear elasticity*. *Comput. Mech.*, 41 (2008) 547–561.
- [38] T.H.H. PIAN AND K. SUMIHARA, *Rational approach for assumed stress finite elements*. *Int. J. Numer. Methods Engrg.*, 20(9) (1984) 1685–1695.
- [39] A. QUARTERONI AND R. RUIZ-BAIER, *Analysis of a finite volume element method for the Stokes problem*. *Numer. Math.*, 118 (2011) 737–764.
- [40] G. ROMANO, F. MARROTTI DE SCIARRA, AND M. DIACO, *Well-posedness and numerical performances of the strain gap method*. *Int. J. Numer. Methods Engrg.*, 51(1) (2001) 103–126.
- [41] R. RUIZ-BAIER AND I. LUNATI, *Mixed finite element – discontinuous finite volume element discretization of a general class of multicontinuum models*. *J. Comput. Phys.*, 322 (2016) 666–688.
- [42] J.C. SIMO AND M.S. RIFAI, *A class of assumed strain method and the methods of incompatible modes*. *Int. J. Numer. Methods Engrg.*, 29 (1990) 1595–1638.
- [43] X. WANG AND K.-J. BATHE, *Displacement/pressure based mixed finite element formulations for acoustic fluid-structure interaction problems*. *Int. J. Numer. Methods Engrg.*, 40 (1997) 2001–2017.
- [44] X. WANG AND K.-J. BATHE, *On mixed elements for acoustic fluid-structure interactions*. *Math. Models Methods Appl. Sci.*, 7(3) (1997) 329–343.
- [45] K. WASHIZU, *Variational Methods in Elasticity & Plasticity*. Pergamon Press, New York, 1982.
- [46] J. WEN, Y. HE, AND J. YANG, *Multiscale enrichment of a finite volume element method for the stationary Navier–Stokes problem*. *Int. J. Comp. Math.*, 90 (2013) 1938–1957.
- [47] Y. WU, X. XIE, AND L. CHEN, *Hybrid stress finite volume method for linear elasticity problems*. *Int. J. Numer. Anal. Model.*, 10(3) (2013) 634–656.

Centro de Investigación en Ingeniería Matemática (CI²MA)

PRE-PUBLICACIONES 2017

- 2017-01 RAIMUND BÜRGER, SUDARSHAN K. KENETTINKARA, DAVID ZORÍO: *Approximate Lax-Wendroff discontinuous Galerkin methods for hyperbolic conservation laws*
- 2017-02 DAVID MORA, GONZALO RIVERA, IVÁN VELÁSQUEZ: *A virtual element method for the vibration problem of Kirchhoff plates*
- 2017-03 CARLOS GARCIA, GABRIEL N. GATICA, ANTONIO MARQUEZ, SALIM MEDDAHI: *A fully discrete scheme for the pressure-stress formulation of the time-domain fluid-structure interaction problem*
- 2017-04 LUIS F. GATICA, FILANDER A. SEQUEIRA: *A priori and a posteriori error analyses of an HDG method for the Brinkman problem*
- 2017-05 ERNESTO CÁCERES, GABRIEL N. GATICA, FILANDER A. SEQUEIRA: *A mixed virtual element method for quasi-Newtonian Stokes flows*
- 2017-06 CELSO R. B. CABRAL, LUIS M. CASTRO, CHRISTIAN E. GALARZA, VÍCTOR H. LACHOS: *Robust quantile regression using a generalized class of skewed distributions*
- 2017-07 RAIMUND BÜRGER, JULIO CAREAGA, STEFAN DIEHL: *A simulation model for settling tanks with varying cross-sectional area*
- 2017-08 RAIMUND BÜRGER, SUDARSHAN K. KENETTINKARA, RICARDO RUIZ-BAIER, HECTOR TORRES: *Non-conforming/DG coupled schemes for multicomponent viscous flow in porous media with adsorption*
- 2017-09 THOMAS FÜHRER, NORBERT HEUER, MICHAEL KARKULIK, RODOLFO RODRÍGUEZ: *Combining the DPG method with finite elements*
- 2017-10 CINTHYA RIVAS, RODOLFO RODRÍGUEZ, MANUEL SOLANO: *A perfectly matched layer for finite-element calculations of diffraction by metallic surface-relief gratings*
- 2017-11 RAIMUND BÜRGER, PEP MULET, LIHKI RUBIO, MAURICIO SEPÚLVEDA: *Linearly implicit IMEX schemes for the equilibrium dispersive model of chromatography*
- 2017-12 VERONICA ANAYA, ZOA DE WIJN, DAVID MORA, RICARDO RUIZ-BAIER: *Mixed displacement-rotation-pressure formulations for elasticity*

Para obtener copias de las Pre-Publicaciones, escribir o llamar a: DIRECTOR, CENTRO DE INVESTIGACIÓN EN INGENIERÍA MATEMÁTICA, UNIVERSIDAD DE CONCEPCIÓN, CASILLA 160-C, CONCEPCIÓN, CHILE, TEL.: 41-2661324, o bien, visitar la página web del centro: <http://www.ci2ma.udec.cl>



**CENTRO DE INVESTIGACIÓN EN
INGENIERÍA MATEMÁTICA (CI²MA)
Universidad de Concepción**



Casilla 160-C, Concepción, Chile
Tel.: 56-41-2661324/2661554/2661316
<http://www.ci2ma.udec.cl>